UAB

Universitat Autònoma de Barcelona

Dipòsit digital de documents de la UAB

Multistimuli-Responsive Fluorescent Switches Based on Spirocyclic Meisenheimer Compounds: Smart Molecules for the Design of Optical Probes and Electrochromic Materials

Marc Villabona,[a] Marina Benet,[a] Silvia Mena,[a] Rabih O. Al-Kaysi,[b] Jordi Hernando[a] and Gonzalo Guirado*[a]*

[a] Departament de Química, Universitat Autònoma de Barcelona, Facultat de Ciències, 08193, Cerdanyola del Vallès, Spain

[b] College of Science and Health Professions, King Saud bin Abdulaziz University for Health Sciences, and King Abdullah International Medical Research Center, Ministry of National Guard Health Affairs, Riyadh 11426, Kingdom of Saudi Arabia.

E-mail: jordi.hernando@uab.cat, gonzalo.guirado@uab.cat

TABLE OF CONTENTS GRAPHIC
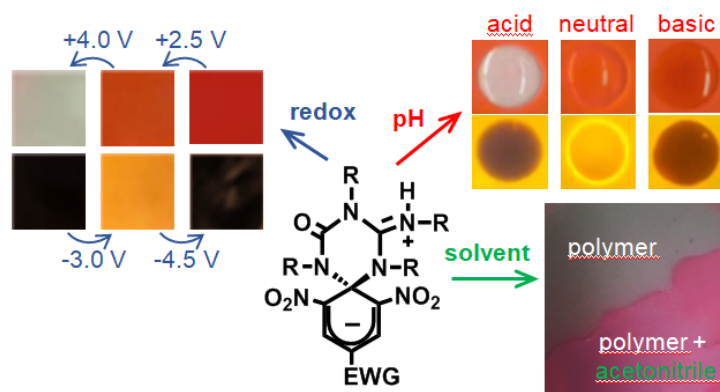
ABSTRACT

Fluorescent switches based on spirocyclic zwitterionic Meisenheimer (SZMC) complexes are stimuli-responsive organic molecules with application in a variety of areas. To expand their functionality, novel switching mechanisms are herein reported for these systems: (a) acid- and redox-triggered formation of an additional protonation state with distinct optical properties, and (b) solvent-induced fluorescence modulation. We demonstrate that these new features, which enable both multistimuli and multistate operation of SZMC switches, can be exploited in the preparation of smart organic materials: wide-range pH optical probes, electrochromic and electrofluorochromic films, and polymer-based fluorescent detectors of organic liquids.

INTRODUCTION

In the last decades fluorescent switches have emerged as smart functional systems with application in a variety of areas, ranging from (bio)chemical sensing[1-4] and imaging[5-8] to information storage,[9,10] processing[11,12] and protection.[13] As such, the development of new molecules and materials enabling stimulus-induced modulation of their emission properties has become an active area of research. Of special interest is the preparation of fluorescent switches capable to respond to two or more different inputs, a multifunctional behavior that can be exploited in complex logic-gate[7,8,14] and analog operations,[15] multimode information storage,[16] smart functional materials[17-22] and multiplexed sensing.[23-25] Most of these fields would also benefit from the development of molecular systems and materials displaying multistate reversible variation of their emission, which should allow for, e.g., increased density of data storage and wider detection ranges for (bio)chemical analytes.[26-30] Therefore, the realization of fluorescent switches with both multistimuli and multistate response capabilities is highly desirable.

A promising class of compounds to reach this behavior are spirocyclic zwitterionic Meisenheimer compounds (SZMC) of 1,3,5-trisubstituted benzene, a family of versatile organic fluorescent switches introduced by us several years ago.[15,31-34] The structure of these systems, inspired from the well-known Jackson-Meisenheimer intermediates of nucleophilic aromatic substitution reactions,[35,36] comprises two different functional units linked through a spiranic carbon atom: (a) a highly fluorescent, visible-light absorbing cyclohexadienyl anion group with strong electron withdrawing substituents at positions 2, 4 and 6, and (b) a triazene ring capable to respond to external stimuli (Scheme 1).[15,31-34]

The use of SZMC switches offers several advantages. Firstly, they can be prepared via a facile one-step synthetic procedure involving commercially available reactants.[15,34,37] Secondly, large emission modulation amplitudes are found between the fluorescent and non fluorescent states of these systems, which in combination with the optical properties of their cyclohexadienyl anion units allow their detection with high sensitivity in the visible region of the spectrum.[15,31-34] Furthermore, they show versatile switching behavior, which can be triggered using different types of stimuli and lead to a multistate scheme. In the case of compound **1** bearing a 2,4,6-trinitrocyclohexadienyl anion, reversible interconversion between its fluorescent (**1b**) and non fluorescent (**1a**) states requires protonation-deprotonation of the guanidine moiety in the triazene ring, which can be achieved either chemically upon acid-base addition or electrochemically by inducing combined electron and hydrogen transfer processes (Scheme 1).[31-33] Additionally, when a trifluoromethyl substituent is introduced in the cyclohexadienyl anion chromophore of **2**, the stability of the spirocyclic protonated state (**2b**) decreases and it can also be thermally converted into a non colored and non fluorescent aromatic compound (**2c**), thus resulting in a three-state switch (Scheme 1).[15]
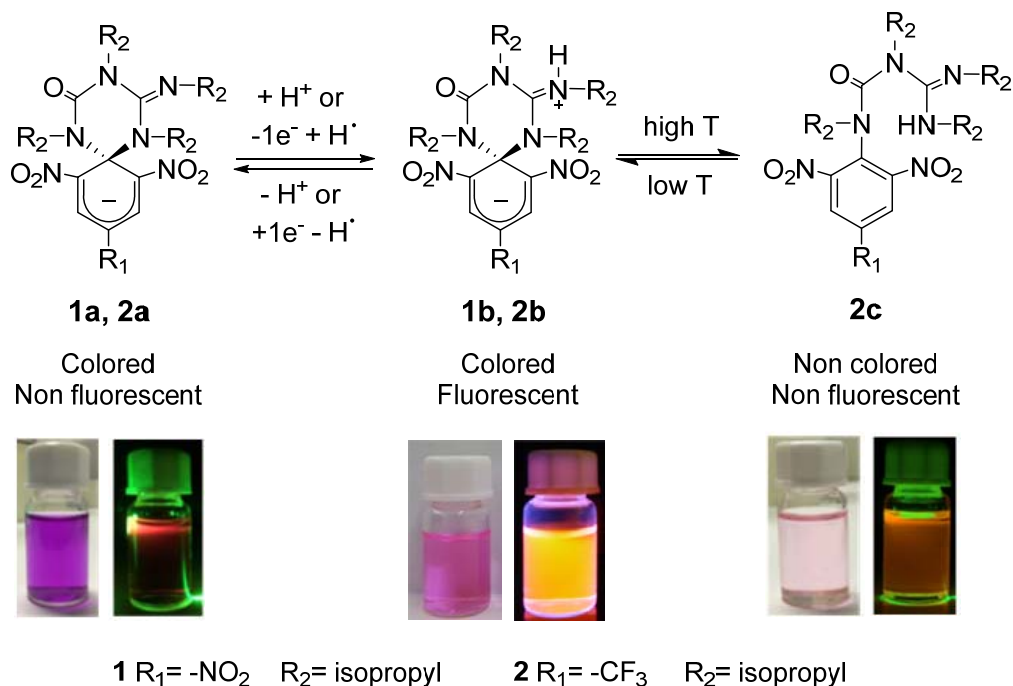
Scheme 1. Multistimuli-responsive behavior of SZMC switches **1**[31-33] and **2**.[15] To illustrate the variation in color and fluorescence emission for the different states of these compounds, photographs are shown of an acetonitrile solution of **2a**, an acetonitrile solution enriched in **2b** at low temperatures, and an acetonitrile solution enriched in **2c** at high temperatures. The residual color and fluorescence emission observed for the latter arise from the presence of a minor fraction of **2b** molecules, which are in tautomeric equilibrium with **2c**.

Because of this combination of properties, SZMCs appear as intriguing multi-addressable organic fluorescent switches that have already been demonstrated to operate on the single molecule level,[32] behave as molecular analogues of field effect transistors,[15] and allow the preparation of nanostructures,[38] invisible security inks,[39] and sensors of ammonia,[39] ions[40,41] and explosives.[42] Aiming to expand their applications, in this work the development of novel interconversion mechanisms for these systems is reported, with which we demonstrate their

unique capacity to behave as both multistimuli-responsive and multistate fluorescent switches, and consequently, to perform as highly versatile chemical sensing platforms and smart materials.

RESULTS AND DISCUSSION

A new protonation state for SZMC switches

As shown in Scheme 1, two different protonation states with distinct optical properties have so far been described for SZMC switches **1** and **2**: an anionic and a zwitterionic state that arise from the acid-base properties of their guanidine group.[15,31-33] In addition, spirocyclic zwitterion **2b** can thermally evolve into neutral aromatic compound **2c**, where the guanidinium moiety of the former converts into a guanidine group upon aperture of the spirocyclic structure of the system.[15] Therefore, **2c** could be further converted into a cationic species by acid-induced protonation of its guanidine group, a process that might also be expanded to switch **1**. Since this would broaden the pH response of SZMC switches in view of chemosensing applications, the protonation of both **1b** and the mixture of neutral tautomers **2b** and **2c** was investigated by ^{1}H NMR in acetonitrile.

Figure 1a plots the room temperature ^{1}H NMR spectra of **1b** upon titration with trifluoroacetic acid (TFA). Clearly, addition of the acid led to a progressive decrement of the intensity of the signals corresponding to the cyclohexadienyl anion protons (δ= 8.83 ppm), the NH group (δ= 4.76 ppm), and the CH (δ= 4.28-3.15 ppm) and methyl protons (δ= 1.67-1.11 ppm) of the isopropyl substituents of **1b**, which completely fainted after titration with 1.2 equivalents of TFA. This, together with the concomitant growth of a novel defined set of resonances, indicated quantitative conversion of the zwitterionic state of the switch into a different compound (**1d**, Scheme 2). While most of the new ^{1}H NMR signals could be assigned to the =C-H (δ= 9.05

ppm) and isopropyl (δ= 4.54-3.77 and 1.33-1.12 ppm) protons of **1d** (Figure 1a), we were particularly intrigued by the broad resonance at δ= 7.25 ppm with an integral of 2H, which resulted from the coalescence of the two other broad downfield-shifted singlets registered at intermediate additions of TFA. Actually, when cooling the protonated sample down to 248 K, the signal at δ= 7.25 ppm split into two separated doublets of equal intensity (Figure 1b), which showed correlation with distinct CH isopropyl protons in the corresponding 2D COSY spectrum (Figure 1c). Therefore, these resonances should correspond to two different NH groups that are directly attached to those isopropyl substituents.
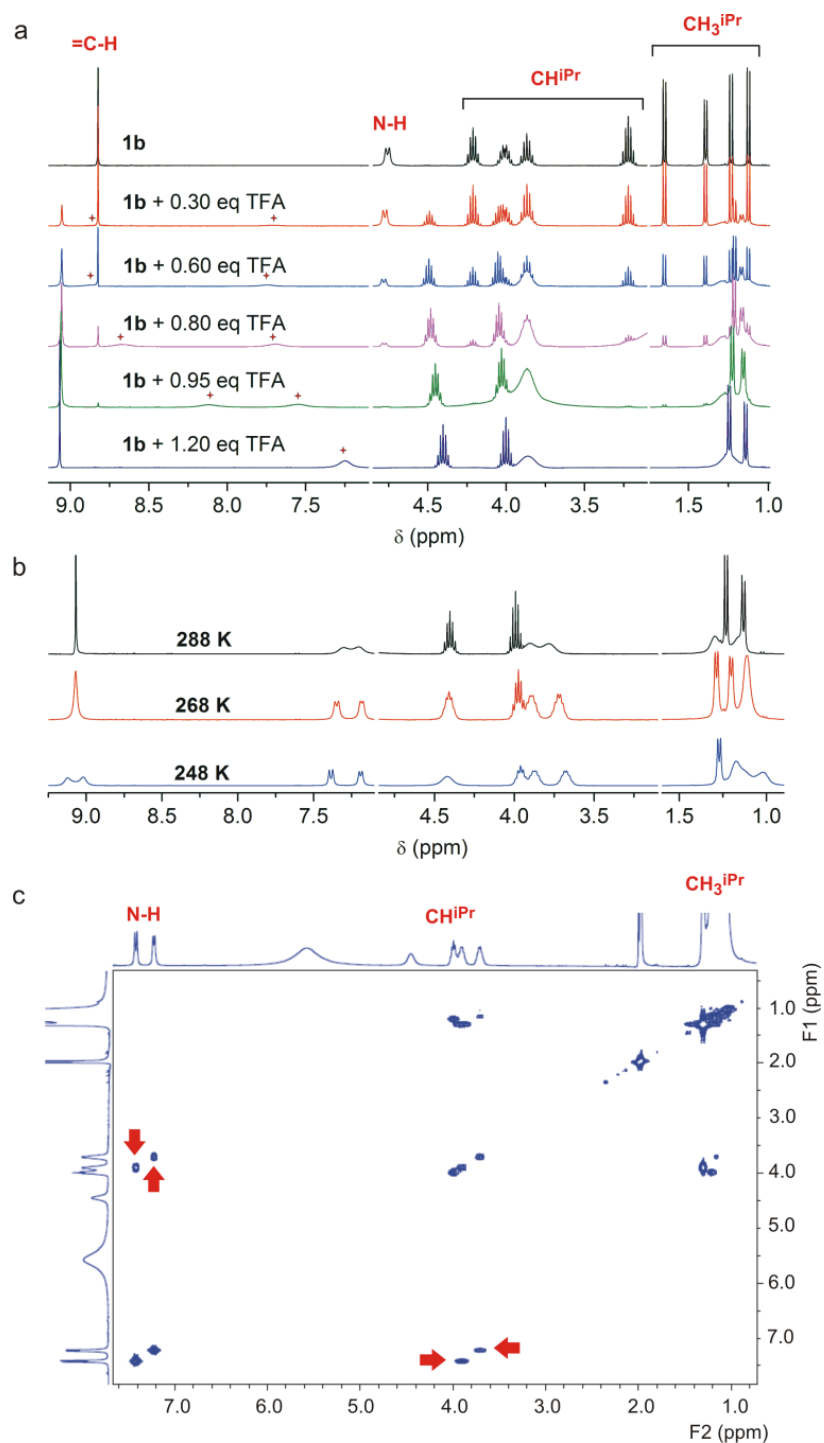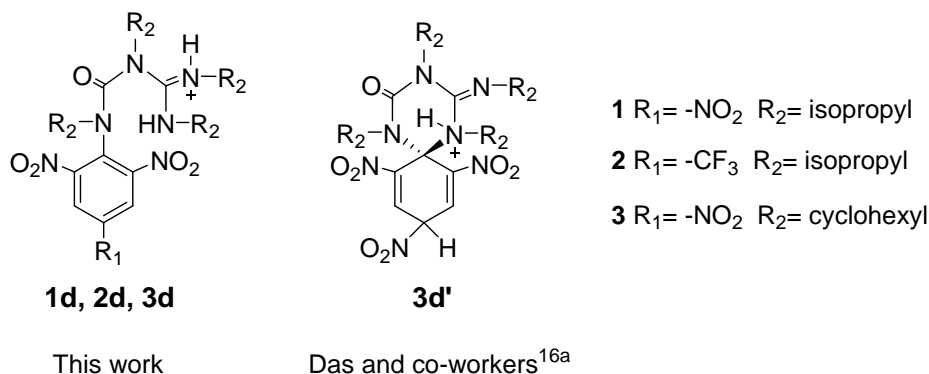
Figure 1. (a) Variation of the ^{1}H NMR (400 MHz, CD$_3$CN, 298 K) spectrum of **1b** upon titration with TFA, which led to the quantitative formation of the protonated state **1d** when 1.20 equivalents of TFA were added. Red stars are used to indicate the growth of two new signals

corresponding to the two NH groups of **1d**, which coalesce upon addition of 1.20 equivalents of TFA. (b) Variation of the ^{1}H NMR (400 MHz, CD$_3$CN) spectrum of **1d** with temperature, which allows resolving the signals for the different NH groups (at δ ~ 7.4 ppm) and isopropyl substituents (at δ ~ 3.7 ppm and δ ~ 1.3 ppm for their CH and CH$_3$ protons, respectively) of the compound. (c) 2D COSY spectrum (400 MHz, CD$_3$CN, 248 K) of **1d**, where cross-peaks are observed between each of the NH resonances at δ ~ 7.4 ppm and one of the isopropyl CH multiplets at δ ~ 3.8 ppm (CH^{iPr}). For sake of clarity, the intensity of the ^{1}H NMR signals in the region 4.8 – 3.1 ppm (x5) and 9.3 – 7.1 ppm (x3) were amplified in the spectra of (a) and (b).

Based on these findings, the structure shown in Scheme 2 is proposed for **1d**, which assumes acid-mediated ring-opening of the spirocyclic backbone of **1b** and protonation of the resulting guanidine group to yield a cationic compound. For such a structure, fast conformational flexibility of the pending chain of the aromatic moiety at room temperature should not only account for the coalescence of the two different NH signals at δ ~ 7.4 ppm, but also of the CH and CH$_3$ resonances of the two terminal isopropyl substituents of the compound, which explains the lower number of signals registered at 298 K for these groups at δ ~ 4.5 – 3.75 ppm and δ ~ 1.5 – 1.0 ppm (Figure 1a). This process was reverted upon cooling and, as a consequence, splitting into separated resonances was also observed for the broad signals of those CH and CH$_3$ protons when lowering the temperature (Figure 1b). In fact, molecular rotation was sufficiently hindered at 248 K as to also make the two aromatic protons of **1d** become anisochronous, as already described for related non spirocyclic compound **2c**.[15]

1 R_1= -NO_2 R_2= isopropyl

2 R_1= -CF_3 R_2= isopropyl

3 R_1= -NO_2 R_2= cyclohexyl

1d, 2d, 3d

This work

3d'

Das and co-workers[16a]

Scheme 2. Structure of the cationic state of SZMC switches established in this work for **1d**, **2d** and **3d**, as well as the structure **3d'** reported by Das and co-workers[39].

Similar results were obtained when investigating the protonation of a tautomeric mixture of **2b** and **2c** with TFA in acetonitrile. Despite the higher complexity of the initial ^{1}H NMR spectrum of this mixture, disappearance of the signals for both neutral **2b** and **2c** compounds and growth of a simpler set of resonances were again observed (Figure S1a). The latter were assigned to protonated state **2d**, the two broad NH signals of which at δ ~ 7.0 ppm did not fully coalesce at room temperature in this case. However, they clearly separated into narrower resonances upon cooling and also showed crossed peaks with CH isopropyl protons in the 2D COSY spectrum (Figure S1b-c). Therefore, these evidences further support our conclusion that the protonation of the neutral state of SZMC switches occurs at their guanidinium group and induces the aperture of their spirocyclic structure (Scheme 2). As such, protonation causes loss of the cyclohexadienyl anion chromophore of this type of switches, which explains the color bleaching observed upon acid addition for both the acetonitrile solutions of **1b** and of the tautomeric mixture **2b**+**2c** in our NMR experiments.

Recently, SZMC switch **3** bearing a 2,4,6-trinitrocyclohexadienyl anion and cyclohexyl substituents was also reported to undergo an interconversion process to a non colored product

10

when its zwitterionic state **3b** was treated with TFA.[39] In this case, however, Das and co-workers ascribed this observation to the formation of the cationic spirocyclic compound **3d'** shown in Scheme 2. Because of the discrepancies between this structure and those proposed in our work for the cationic state of SZMC switches, we also investigated the protonation of **3b** by ^{1}H NMR. A detailed description of the results obtained in these experiments are given in the Supporting Information (Figures S2 and S3), where crossed peaks between two distinct NH resonances and cyclohexyl signals were observed for **3b**. This finding allows disambiguation of the actual structure of the cationic state of the system: the new proton introduced cannot be attached to the unsaturated ring of the compound, but it must lie next to one of the pending alkyl chains (**3d**), as proposed in our work for other SZMC switches and in contrast to the assignment of Das and co-workers[39] (**3d'**, Scheme 2).

SZMC switches as wide range pH probes

Once uncovered the nature of the cationic state of SZMCs, we investigated the pH-induced optical switching behavior expected for compounds **1** and **2** upon protonation of their neutral form. Figure 2a-b shows the variation in the absorption and emission spectra of **1b** and of the tautomeric mixture **2b**+**2c** in acetonitrile upon acid addition. Although $HClO_4$ was preferably used in these experiments because it is a strong acid in acetonitrile,[32] identical results were achieved when employing a non oxidizing acid such as TFA. In both cases, continuous decrease of the visible absorption and emission signals of both compounds was observed by protonation, as previously described for **3b**[39] and in agreement with the loss of the chromophoric cyclohexadienyl anion core in **1d** and **2d**. It must be noted that acid-induced conversion of the neutral state of **1** into its cationic counterpart yielded defined isosbestic points in the UV-vis spectra. In accordance to ^{1}H NMR data, this suggests that protonation of **1b** and of the mixture

2b+**2c** occurs without apparent degradation. Eventually, quantitative conversion of these compounds into **1d** and **2d** was observed, as demonstrated by the complete suppression of the color and fluorescence emission of the initial solutions of their neutral state. More importantly, we found this process to be fully reversible by addition of tetrabutylammonium hydroxide (TBAOH) as a base, which proved the capacity of SZMC switches to recover their spirocyclic structure after adjusting the acidity of the medium (i.e. the acid-base nature of such transformation). This is unambiguously demonstrated by Figure 2c, which plots the robust and reproducible fluorescence switching operation registered for **1** and **2** upon repetitive acid-base cycles.
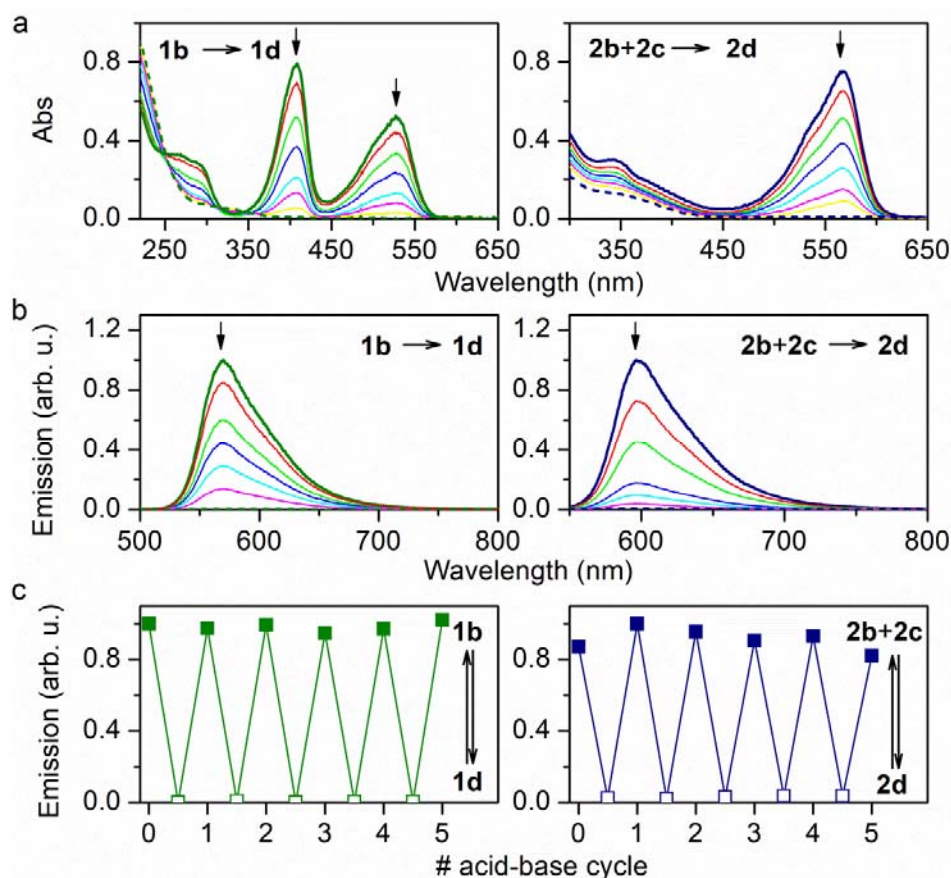
Figure 2. (a-b) Acid-base interconversion between **1b** and **1d** as well as between the tautomeric mixture **2b**+**2c** and **2d** monitored by (a) UV-vis absorption spectroscopy (c_{1b} = 6.0x10^{-5} M, c_{2b+2c} = 2.0x10^{-4} M, acetonitrile, 298 K), and (b) fluorescence spectroscopy (c_{1b} = 1.5x10^{-5} M, c_{2b+2c} = 4.0x10^{-5} M, acetonitrile, λ_{exc}= 473 nm for **1** and 532 nm for **2**, 298 K). In each case increasing amounts of HClO$_4$ were added until reaching *ca*. 1 equivalent of acid. (c) Variation of the emission intensity during 5 consecutive cycles of acid-base switching between **1b** and **1d** as well as between the mixture **2b**+**2c** and **2d**, using HClO$_4$ and TBAOH as acid and base, respectively. The fluorescence of the neutral states of these compounds is shown in hollow symbols, while solid symbols are used for their cationic forms.

Based on the capacity of SZMCs to reversibly interconvert between three different protonation states with distinct optical properties, they could be envisaged as wide range acidity probes[28,43,44] responding to both low and high pH values. As a proof of concept of this behavior, we focused our attention on **1**, since it only presents a colored, fluorescent zwitterionic form in the neutral state of the system, thus increasing the contrast in optical properties upon switching. For this compound, the variation in visible light absorbance and emission was measured as a function of pH in acetonitrile (Figure 3a), which was taken as the solvent for these studies because of: (a) the low solubility of **1** in aqueous media, which resulted in additional, more intricate optical changes due to dye aggregation; (b) the practical interest of pH determination in organic solvents for a wide range of applications.[45-47] From our experiments, the pKa constants for the acid-base equilibria of **1** in acetonitrile could be determined: pKa = 15.8 ± 0.1 and 21.2 ± 0.1 for the **1d**→**1b** and **1b**→**1a** interconversion processes, respectively. Since the autoprotolysis constant of acetonitrile is pK^{ACN} ≥ 33, the pH scale in acetonitrile spreads over a much larger range than in water (typically, pH ~ 1-33).[48] As such, the pKa values determined for **1d** and **1b**

indicate that both compounds behave as weak acids in acetonitrile and undergo deprotonation at rather different pH windows. Therefore, the changes in optical properties that concomitantly occur could be used for pH sensing over a large range.
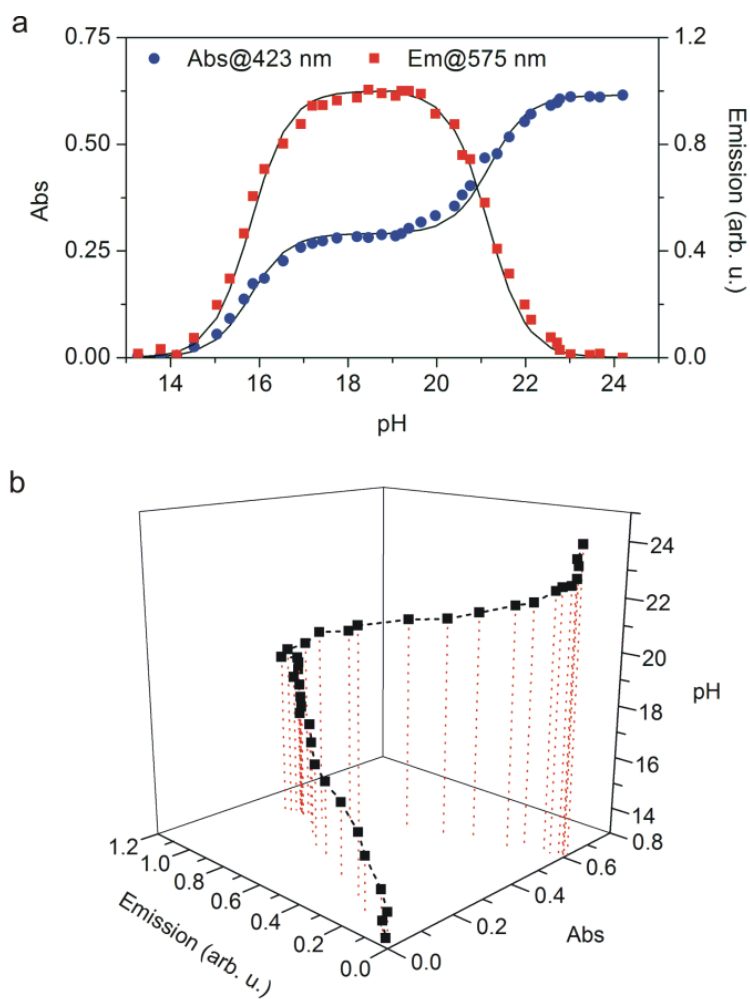

Figure 3. (a) pH dependence of the absorption at 423 nm and of the fluorescence emission intensity at 575 nm for **1** in acetonitrile ($c_1 = 4.4\text{x}10^{-5}$ M, $\lambda_{exc}= 473$ nm, 298 K). Variation of pH was achieved by addition of $HClO_4$ and TBAOH. Symbols correspond to experimental data, while solid lines plot the simulated absorption and emission signals that were computed from the pKa constants, extinction coefficients and fluorescence quantum yields determined for **1**. (b) 3D

plot showing the correspondence between pH and the absorption and fluorescence signals measured at 423 nm and 575 nm, respectively, for **1** in acetonitrile.

In the case of the pH-dependent fluorescence response of **1**, it follows a symmetric "off-on-off" behavior (Figure 3a), since the neutral state **1b** is the single emissive species of the system and it is only predominant for intermediate values of pH (in the case of acetonitrile solutions, for pH ~ 16-21). On the other hand, by properly selecting the detection wavelength (e.g. λ = 423 nm), a stepwise "off-on$_1$-on$_2$" profile can be obtained for the variation of the absorption signal owing to the different absorption spectra of **1a** and **1b** in the visible region (Figure 3a), which resembles the behavior described for other compounds proposed for ternary molecular logic.[49,50] Because of the complementarity of these "off-on-off" and "off-on$_1$-on$_2$" optical responses, a univocal value of pH can be retrieved from each pair of absorption and fluorescence values measured upon acid or base addition over acetonitrile solutions of **1**, as shown by the 3D representation in Figure 3b. Therefore, this demonstrates that **1** operates as a pH optical probe over a large interval, which in the case of acetonitrile media covers about 10 pH units (pH ~ 14-24). Importantly, this behavior could not only be extended to other SZMCs with three-state switching capabilities, but also modulated by tuning the pKa constants of their pH-active guanidine group upon variation of the appended substituents.

Wide range pH optical detection using SZMC switch **1** could be transferred from solution to the solid state by simply dispersing this halochromic molecule in a polymer matrix. In particular, a polymethyl methacrylate (PMMA) thin film was prepared and loaded with **1b**, and then exposed to acid, neutral and basic acetonitrile solutions (Figure 4). When a droplet of acetonitrile was deposited onto the polymer film, we observed no variation of the optical properties of the

loaded **1b** molecules. By contrast, changes in the color and fluorescence of the PMMA sample were registered when brought in contact with a 0.1 M TFA and a 0.1 M TBAOH acetonitrile solution, which were consistent with acid-induced **1b→1d** (i.e. color bleaching and emission quenching) and base-induced **1b→1a** (i.e. color variation and emission quenching) interconversion, respectively. This conclusion was corroborated by control experiments on pure, non doped PMMA films, which were transparent and non fluorescent and did not show any variation of their optical properties upon exposure to acid, neutral and basic acetonitrile solutions (Figure S4).
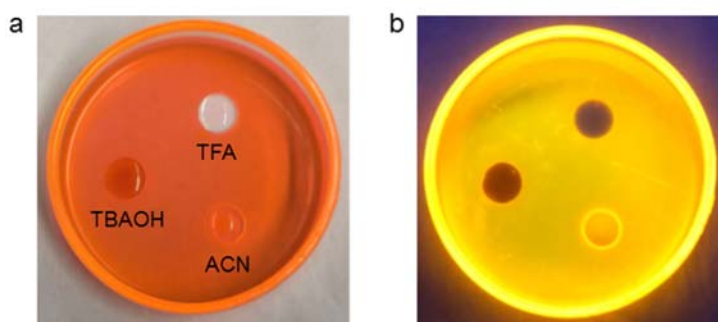

Figure 4. Photographs of a PMMA film loaded with **1b** molecules onto which droplets of 3 different solutions were deposited: acetonitrile (ACN), a 0.1 M TFA acetonitrile solution (TFA), and a 0.1 M TBAOH acetonitrile solution (TBAOH). Changes in color and fluorescence are observed in (a) and (b), respectively. The image in b) was taken in the dark and under irradiation with a 365 nm lamp.

Extended redox switching of SZMCs: preparation of electrofluorochromic materials

An added advantage of SZMCs over other pH-responsive fluorescent switches is their capacity to undergo redox-induced interconversion between their anionic and neutral states in

organic solvents such as acetonitrile or DMF.[15,32-34] Inspired by this behavior, we explored herein the reversible transformation between the neutral and cationic forms of these compounds by means of electrochemical stimuli. Because of its simpler switching scheme owing to the thermal stability of its zwitterionic state, we took compound **1** as a benchmark case for these studies.
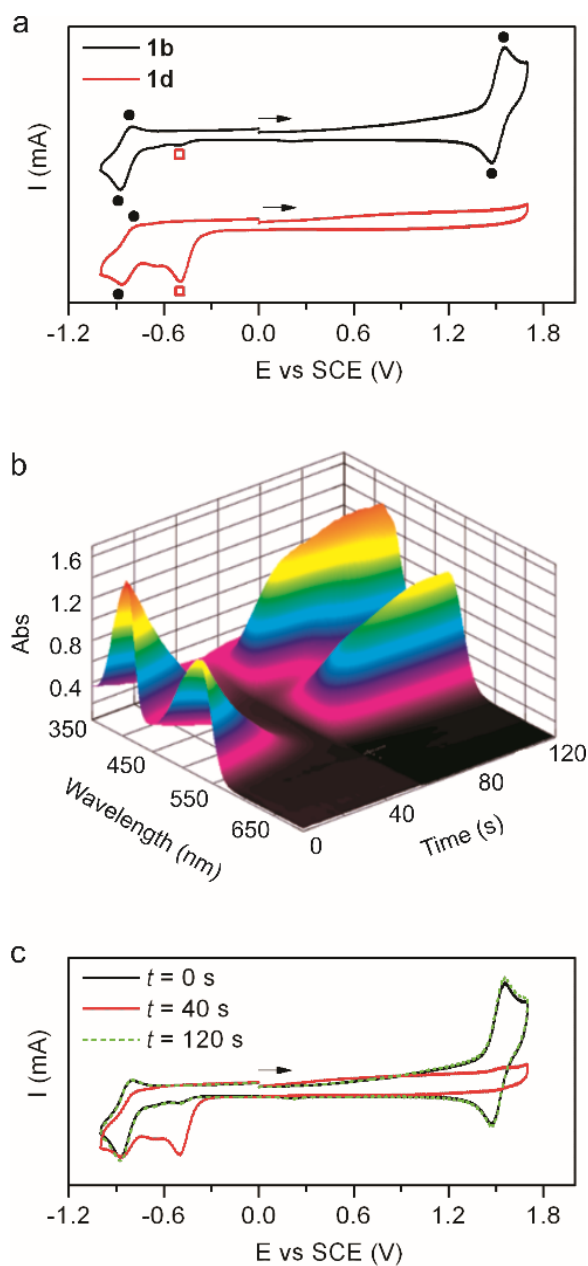
Figure 5. (a) Cyclic voltammograms of **1b** and **1d** in acetonitrile at 298 K (c = 5.0x10^{-4} M, 0.1 M n-Bu$_4$NPF$_6$, scan rate = 0.5 V s^{-1}). Solid circles and hollow squares are used to assign the electrochemical waves arising from **1b** and **1d**, respectively. (b) Variation of the absorption spectra of **1b** in acetonitrile at 298 K when the following sequence of electrochemical potentials was applied: $E_{applied}$ = +1.7 V (vs SCE) from t = 0-40 s and $E_{applied}$ = -0.6 V (vs SCE) from t = 40-120 s (c = 5.0x10^{-4} M, 0.1 M n-Bu$_4$NPF$_6$). (c) Cyclic voltammograms registered at different times (t = 0, 40 and 120 s) for the sample subjected to the spectroelectrochemical experiment shown in (b) (scan rate = 0.5 V s^{-1}). Arrows in (a) and (c) indicate the direction of the potential scan in each case.

Figure 5a plots the cyclic voltammograms of **1b** and **1d** in acetonitrile, an aprotic solvent with well-known hydrogen atom donor properties in electrochemical reactions.[51] As already reported, zwitterion **1b** shows two characteristic redox waves: a one-electron reversible oxidation wave at E^0 = +1.52 V (vs SCE), and a one-electron pseudoreversible reduction wave at $E_{p,c}$ = -0.85 V (vs SCE), which was proven to lead to the formation of anion **1a** after hydrogen transfer from the solvent to the radical anion **1b**$^{\bullet-}$ generated electrochemically (Scheme 3a).[32,33] Under the same experimental conditions, no oxidation wave was registered for **1d**, whereas two different one-electron reduction waves were observed at $E_{p,c}$ = -0.50 and -0.85 V (vs SCE). Two aspects must be particularly noted about these waves. On one hand, the second pseudoreversible wave at -0.85 V (vs SCE) resembles that measured for **1b**, which suggests that the first irreversible reduction process of **1d** at lower potentials (-0.50 V (vs SCE)) couples to a hydrogen atom loss chemical reaction that would result in product deprotonation and formation of the zwitterionic state of the switch. On the other hand, a very low intensity irreversible reduction wave at -0.50 V (vs SCE) could also be detected in the cyclic voltammogram of **1b**. In view of the electrochemical data

registered for **1d**, this could be an indication that the previously scanned oxidation wave of **1b** at +1.52 V (vs SCE) was not fully reversible at this cyclic voltammogramm scale time and it led to the generation of a small amount of the cationic state of the system.

Prompted by these results, we assayed the redox interconversion between the neutral and cationic forms of **1** using oxidative (to induce **1b** → **1d** transformation) and reductive (to induce **1d** → **1b** transformation) controlled potential electrolysis, which were monitored by means of spectroelectrochemical and cyclic voltammetry measurements. Figure 5b shows the variation in absorption spectra measured for **1b** in acetonitrile when subjecting this sample to consecutive oxidative ($E_{applied}$= +1.7 V (vs SCE) for 40 s) and reductive ($E_{applied}$= -0.6 V (vs SCE) for 80 s) potentials, while the corresponding cyclic voltammograms at *t* = 0, 40 and 120 s are shown in Figure 5c. Clearly, oxidation of **1b** resulted in decoloration of the sample and formation of the same type of cyclic voltammogram previously registered for **1d**. Hence, this reveals that, upon one-electron oxidation of **1b**, its radical cation abstracts a hydrogen atom from the solvent and undergoes ring opening of its spirocyclic motif, thus generating **1d** (Scheme 3b). In addition, subsequent reduction of **1d** allowed the absorption spectrum and the cyclic voltammogram of **1b** to be recovered, which suggests that **1d**• releases a hydrogen atom that may eventually evolve into molecular hydrogen[52] and is then capable to retake the spirocyclic structure of SZMC systems (Scheme 3b). In combination with previous reported data[32,33] and the results shown in the previous sections, this demonstrates that **1** operates as a multistate and a multiresponsive fluorescent switch, since it interconverts between its anionic, neutral and cationic forms through both acid-base and redox stimuli, a behavior also expected for other SZMCs. It must be noted that such diverse types of stimuli produce the same molecular effects (i.e. protonation and deprotonation of the switches) and, as a consequence, identical variation of their optical

properties. Therefore, no changes in molecular response must be expected if a combination of acid-base and redox stimuli are used and, indeed, combined chemical-electrochemical operation of these compounds could be achieved.
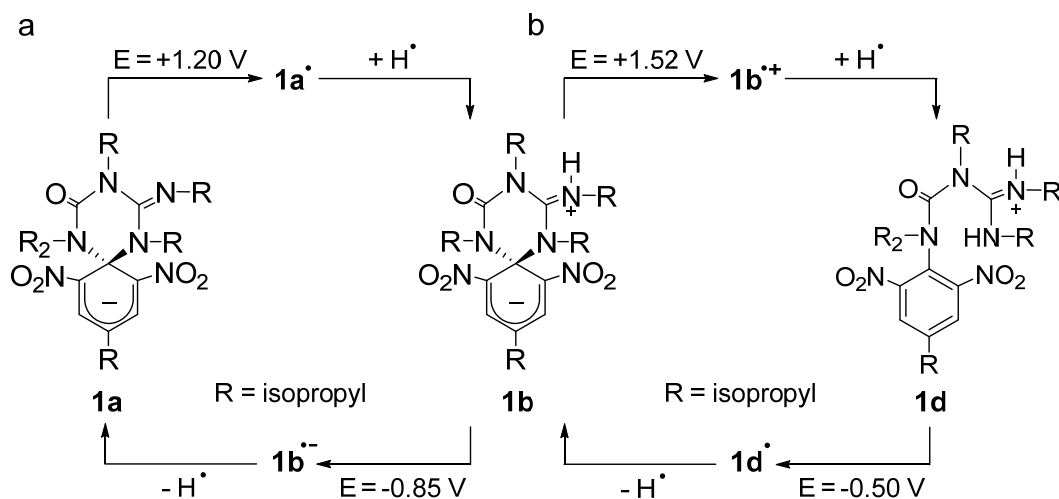
Scheme 3. (a) Redox-induced interconversion between the anionic and zwitterionic states of **1**.[32,33] (b) Redox-induced interconversion between the zwitterionic and the cationic states of **1** in acetonitrile, which involves separate electron and hydrogen atom transfer steps. Based on previous works,[32,51,52] we postulate that **1b**•+ must abstract a hydrogen atom from acetonitrile, while the hydrogen atom released by **1d**• should eventually evolve into molecular hydrogen. All potentials given are referred to SCE.

The capability of **1** to switch electrochemically between states with different absorption and fluorescence properties could be exploited in the preparation of electrochromic and electrofluorochromic devices. To illustrate this behavior, we loaded **1b** into ion gels prepared by mixing an ionic liquid (1-butyl-3-methylimidazolium bis(trifluoromethylsulfonyl)imide, [BMIM][TFSI]) and a polymer (poly(vinylidene fluoride-co-hexafluoropropylene, P(VDF-co-

HFP)).[53] As shown in Figure 6a-b, this resulted in the formation of a slightly conductive elastic gel (conductivity = 0.686 mS cm^{-1} at room temperature) that conserved the color and emissive behavior of the embedded spirocyclic zwitterionic molecules. Later, thin films of this gel (~ 1 mm in thickness) were placed between two ITO-coated glass slides and different electric potentials were applied to induce the conversion between **1b** and **1a** as well as between **1b** and **1d**. Although large potentials were required due to the poor conductivity of the ion gels obtained, changes in color and fluorescence emission were registered that revealed successful redox-triggered transformation between the different states of **1**. Thus, by applying a reduction potential at -4.5 V and a subsequent oxidation potential at +2.5 V, we achieved reversible interconversion between the fluorescent **1b** and non fluorescent **1a** forms of the switch (Figure 6c). In addition, transformation between **1b** and **1d** could also be accomplished within the ion gel applying an oxidation potential at +4.0 V and a reduction potential at -3.0 V, thus resulting in reversible decoloration and loss of fluorescence of the material (Figure 6d-e). In this case, however, these effects could not be fully achieved in certain regions of the gel, which we associated to those with lower conductivities and/or higher thicknesses. In spite of this, these exploratory experiments demonstrate the capacity to construct electrochromic and electrofluorochromic devices based on compound **1** and other SZMC switches.
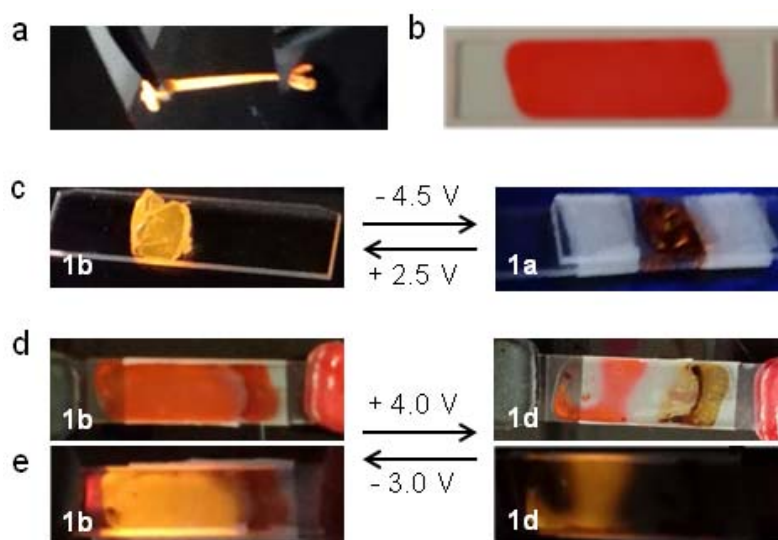
Figure 6. (a-b) Photographs of ion gels prepared from [BMIM][TFSI], P(VDF-co-HFP) and **1b**. In (a) one of the ion gels prepared was pulled and irradiated in the dark with a UV lamp (365 nm) to illustrate its elastic and fluorescent behavior. The color of another ion gel deposited onto an ITO-coated glass plate is shown in (b). (c) Photographs of one of these gels before and after redox-induced interconversion between **1b** and **1a**. Both images were taken in the dark and under irradiation with a 365 nm lamp to demonstrate the change in emission resulting from the transformation between **1b** and **1a**. (d-e) Photographs of another gel before and after redox-induced interconversion between **1b** and **1d**. To monitor both the changes in color and fluorescence arising from this process, images were taken (d) under daylight and (e) under irradiation at 365 nm in the dark. The brown substance observed in (d) upon application of +4.0 V corresponds to ferrocenium ions, which were formed by oxidation of 1,1'-dimethylferrocene molecules previously added to the ion gel as a redox reference system.

Solvent-induced switching of SZMCs

SZMC **2** bearing a 2,6-dinitro-4-(trifluoromethyl)cyclohexadienyl anion chromophore shows temperature-controlled fluorescent switching due to the tautomeric equilibrium between its

emissive spirocyclic zwitterionic state and its non emissive aromatic neutral form (Scheme 1).[15] A similar behavior could also be accomplished by changing the surrounding environment, since different solvation effects on the relative stability of both states are expected owing to their different charge distribution. In view of this, we explored the solvent-induced fluorescence switching of **2**.

First, we investigated the variation with solvent of the equilibrium concentration ratio between **2b** and **2c** by ^{1}H NMR. By separately integrating the low field signals of these compounds (Figure S5), the molar fraction of the fluorescent isomer **2b** (χ_{2b}) in the neutral state of the switch could be estimated for different organic media and temperatures (Figure 7a). This allowed unraveling dramatic solvent effects on the tautomeric equilibrium constant of the neutral state of **2**, which should enable large modulation of the **2b:2c** concentration ratio by simply replacing the surrounding media. For instance, while **2b** concentration in toluene fell below the detection limits of ^{1}H NMR for the three temperatures considered, molar fraction values higher than 0.30 were found for this compound in other organic solvents such as CHCl$_3$ and acetonitrile at 273 K. In addition, the thermal dependence of χ_{2b} was also observed to critically depend on the solvent of choice; e.g. a 33-fold decrease in **2b** molar fraction was measured in CHCl$_3$ when heating from 273 to 313 K, whereas it remained almost unaltered for THF within the same temperature range.

All these results can be rationalized on the basis of different factors. On one hand, polarity increases the relative concentration of tautomer **2b** in aprotic media, as expected due to the zwitterionic nature of this product. Accordingly, relatively large χ_{2b} values were measured in acetonitrile and DMSO even when heating. In addition, the capacity of the solvent molecules to

stabilize the guanidinium group of isomer **2b** via hydrogen bond interactions does play a role in aprotic media, thus accounting for the lower thermal decrement of χ_{2b} observed in THF, acetone, acetonitrile and DMSO with respect to toluene, CH_2Cl_2 and $CHCl_3$. On the other hand, dissolution in polar protic solvents (e.g. methanol) significantly promotes the formation of the non zwitterionic species, thus leading to relatively low χ_{2b} values regardless of the temperature. Although the actual mechanism underlying this behavior is unclear to us, we hypothesize that hydrogen bonding interactions of the nitrogen atoms next to the spiro carbon atom with solvent molecules reduces the stability of the cyclic structure of **2b** and favors ring opening to yield **2c**.
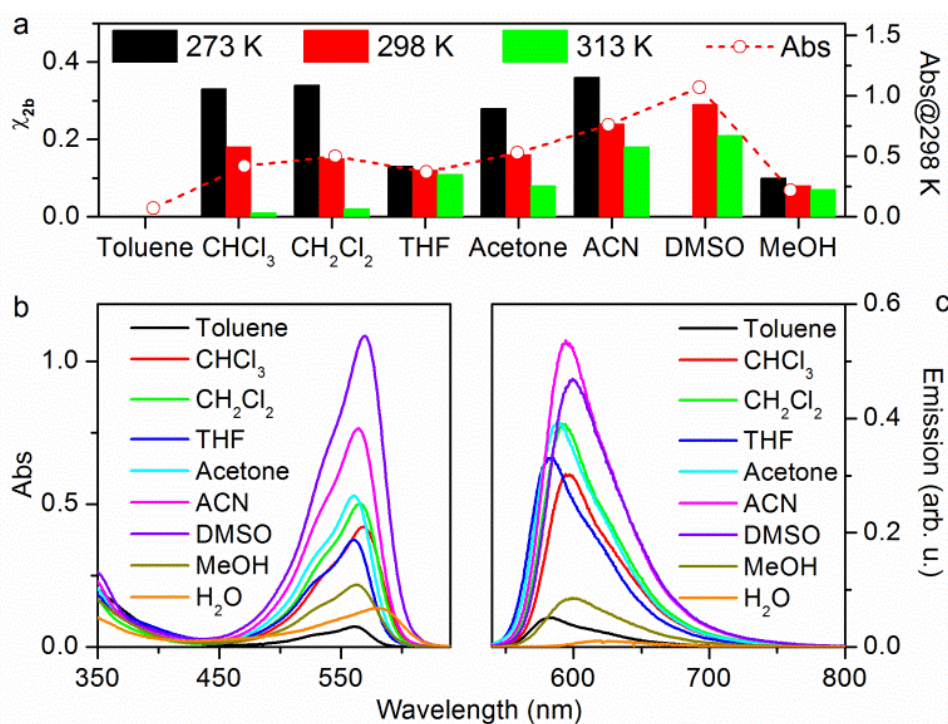

Figure 7. (a) Molar fractions of compound **2b** in the equilibrium tautomeric mixture of the neutral state of the switch for different solvents and temperatures, as determined from ^{1}H NMR. The χ_{2b} value for DMSO at 273 K could not be determined because this temperature falls below the melting point of the solvent. In addition, the absorbances at the spectral maxima are also

given for 2.1×10^{-4} M solutions of the tautomeric mixture **2b**+**2c** in each solvent at 298 K. (b) Absorption spectra of the tautomeric mixture **2b**+**2c** in different solvents and at 298 K (c_2 = 2.1×10^{-4} M). (c) Fluorescence emission spectra of the tautomeric mixture **2b**+**2c** in different solvents and at 298 K (c_2 = 4×10^{-5} M, λ_{exc} = 532 nm).

Because of the different optical properties of tautomers **2b** and **2c**, modulation of their concentration ratio with solvent should result in concomitant changes in absorption and emission. Indeed, when optically characterizing the equilibrium mixture **2b**+**2c** in different solvents at 298 K, large intensity variations were measured for the absorption and fluorescence signals in the visible region selectively arising from **2b** (Figure 7b-c). In the case of the absorption data, they fairly reproduced the trends already inferred from ^{1}H NMR measurements (Figure 7a), the maximum and minimal signals being registered for DMSO and toluene, respectively. This suggests little variation of the extinction coefficients of **2b** with solvent, which makes the overall absorption signal of the equilibrium mixture **2b**+**2c** mainly depend on χ_{2b} for each solvent and temperature of interest. By contrast, non negligible solvatochromic effects were observed for the absorption spectrum of **2b** ($\lambda_{abs,max}$=560 and 581 nm for toluene and water, respectively; Figure 7b), which indicates differential solvation of its ground and first-excited states.[54] It must be mentioned that, in the case of water, rather low visible light absorption was registered. Although χ_{2b} could not be measured in this solvent by ^{1}H NMR because of limited solubility, this observation further supports the poor stability established for the colored state **2b** in protic solvents on the basis of the NMR experiments conducted in methanol.

Similarly, large solvatofluorochromic effects were measured for **2b**, the emission spectra of the mixture **2b**+**2c** bathochromically shifting with solvent polarity ($\lambda_{fl,max}$=581 and 605 nm for

toluene and DMSO, respectively; Figure 7c). In spite of this, minimal variations of the fluorescence quantum yield (Φ_{fl}) of **2b** were mainly registered, and high $\Phi_{fl,\textbf{2b}}$ values (>0.65) were determined for all the apolar and polar aprotic solvents considered (Table S1). As a result, the fluorescence intensities measured for the equilibrium mixture **2b**+**2c** in those cases essentially depended on the actual concentration of the emissive state **2b** (Figure 7c). For protic solvents such as methanol and water, however, a clear decrease in $\Phi_{fl,\textbf{2b}}$ was observed (< 0.40, Table S1), which in combination with the low $\chi_{\textbf{2b}}$ also measured in these media resulted in rather weak emission intensities (Figure 7c).

Owing to the solvent variation of χ_{2b} and $\Phi_{fl,2b}$, the equilibrium mixture **2b**+**2c** could be employed as a fluorescent probe of organic liquids and vapors. As a proof of concept, we explored its application to the fluorescence detection of acetonitrile, since maximal emission intensity was registered in this solvent for the neutral state of **2** at room temperature due to the large stability and fluorescence quantum yield of tautomer **2b**. As a consequence, if this compound is dissolved in organic media where **2b** presents low stability (e.g. toluene) and/or low fluorescence quantum yield (e.g. water), the addition of increasing amounts of acetonitrile should result in a large increase in emission intensity, as experimentally demonstrated in Figure 8a-b. Aiming at reproducing this behavior in solid materials that could be applied in functional devices, the tautomerix mixture **2b**+**2c** was embedded in thin films of polystyrene (PS) and polyvinyl alcohol (PVA). In both cases, dimly colored and fluorescent polymer films were obtained due to the low stability of **2b** in apolar (PS) and protic (PVA) media as well as to the reduced Φ_{fl} of this compound in protic environments (PVA, Figure 8c-d). Interestingly, strong coloration of the films and dramatic enhancement of their emission intensity were observed upon

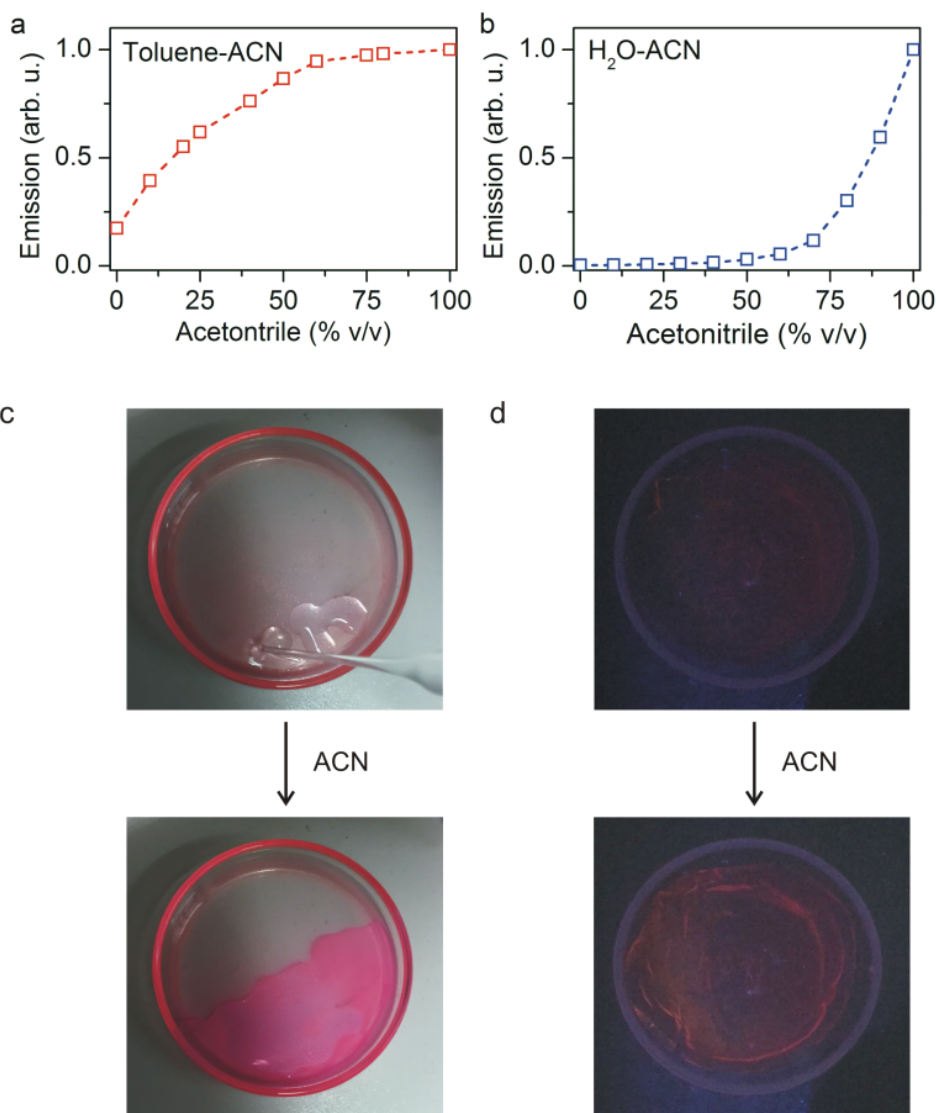swelling with acetonitrile, thus enabling the fluorescence detection of this chemical species (Figure 8c-d).

Figure 8. (a-b) Variation of the emission intensity of the tautomeric mixture **2b**+**2c** in toluene-acetonitrile and water-acetonitrile mixtures at 298 K (c_2 = 4x10^{-5} M, λ_{exc} = 532 nm). (c) Photographs of a PS film doped with the tautomeric mixture **2b**+**2c** before and after swelling with acetonitrile. For sake of comparison, acetonitrile was only poured onto one half of the

polymer film. (d) Photographs of a PVA film doped with the tautomeric mixture **2b**+**2c** before and after swelling with acetonitrile. These images were taken in the dark and under irradiation with a 365 nm lamp.

CONCLUSIONS

Novel optical switching mechanisms are described in this work for spirocyclic Meisenheimer complexes, an intriguing family of stimuli-responsive fluorescent molecules. On one hand, a new protonation state with distinct optical properties has been elucidated for these compounds, which can be obtained chemically in acidic media and electrochemically upon oxidation of the zwitterionic form of SZMC switches. This behavior has been exploited in the preparation of wide-range pH probes and electrochromic and electrofluorochromic materials. On the other hand, solvent-induced fluorescence modulation has also been proven for SZMCs bearing a trifluoromethyl substituent in their cyclohexadienyl anion chromophore. This enables their use for the fabrication of detectors of organic liquids and vapors. Our work therefore demonstrates the capability of spirocyclic Meisenheimer compounds to operate as multistimuli-responsive and multistate fluorescent switches, which makes them highly versatile platforms for the design of chemical sensors and smart materials.

EXPERIMENTAL SECTION

Materials

Organic solvents used in the synthesis were distilled over CaH_2 and stored over activated molecular sieves (3 Å). Spectroscopic grade solvents were used as received. All chemicals used for the synthesis were of reagent grade with > 98% purity and they were used without further

purification. Flash column chromatography was performed on silica gel 60 Å with average particle size 35-70 μm.

NMR spectroscopy

^{1}H NMR spectra were recorded on Bruker DPX360 (360 MHz) and Bruker AV-III400 (400 MHz) spectrometers. Proton chemical shifts are reported in ppm (δ) and are referenced against solvent residual signals. Coupling constant values (J) are reported in Hz.

Optical characterization

UV-vis absorption spectra were recorded using a HP 8452A spectrophotometer (Agilent) with Chemstation software. Fluorescence spectra were recorded by means of a custom-made spectrofluorometer using cw lasers (BeamQ, λ_{exc} = 473 nm; Z-laser, λ_{exc} = 532 nm) as excitation sources. Emitted photons were detected using an Andor ICCD camera coupled to a spectrograph. All the emission spectra registered were corrected by the wavelength dependence of the spectral response of the detection system. In all the cases spectroscopic quality solvents and 1-cm quartz cuvettes were used. Temperature was controlled using a refrigerated circulator bath (Huber MPC-K6) connected to the sample holder. Fluorescence quantum yields were determined using the standard method[55] for highly diluted solutions of the compounds of interest to prevent self-absorption processes (absorption < 0.05 at the excitation wavelength) and relative to *N,N'*-bis(1-hexylheptyl)perylene-3,4,9,10 tetracarboxybismide in acetonitrile (Φ_{fl}=1[56]) or *N,N'*-bis(butyl)-1,6,7,12-tetra-(4-*tert*-butylphenoxy)perylene-3,4:9,10-tetracarboxylic diimide in CH_2Cl_2 (Φ_{fl} =1[57]). The same excitation wavelength was used for both the sample of interest and the standard in all these measurements.

Electrochemical characterization and switching

Cyclic voltammograms were registered using a VSP100 BIOLOGIC potentiostat and a conical electrochemical cell equipped with an argon bubbling source for degassing, a glassy carbon working electrode (WE, d= 0.45 mm), a glassy carbon auxiliary electrode (CE, d= 3 mm) and a saturated calomel reference electrode (SCE, RE). All the potentials are reported versus a SCE isolated from the working electrode by a salt bridge. All measurements were performed in acetonitrile solution containing 0.1 M of n-Bu$_4$NPF$_6$ as a supporting electrolyte. Electrolysis experiments at controlled potentials were undertaken with a EG&G Princeton Applied Research (PAR) 273A potentiostat and an electrochemical cell equipped with an argon bubbling source, a carbon graphite rod, an auxiliary platinum electrode and a SCE reference electrode. All experiments were performed in acetonitrile solutions containing n-Bu$_4$NPF$_6$ (0.1 M) as a supporting electrolyte. The products obtained were then characterized by ^{1}H NMR, cyclic voltammetry, UV-Vis absorption spectroscopy and fluorescence spectroscopy. Spectroelectrochemical experiments were performed in a 1-mm thin layer quartz glass cell using platinum gauze and platinum wire as working and counter electrodes, respectively, whereas a saturated calomel electrode (SCE) was used as a reference electrode. A PC-controlled VSP-Potentiostat synchronized with an MMS-UV-Vis high speed diode array spectrometer with a bandwidth of 330-1100 nm and a deuterium/tungsten light source (HM) and optical fiber (SMA, J&M) was employed to register the spectroelectrochemical measurements. Each spectrum was recorded after 0.05 s. BioKine32 software was used for data acquisition and treatment.

pH measurements

pH measurements upon acid-base addition on acetonitrile solutions of **1** were performed at room temperature with a Crison 5028 pH electrode in a Crison BASIC 20+ potentiometer. pH values are given relative to the acetonitrile solvent (^s_spH scale).[58] To calibrate the electrode

system we used reference buffers in acetonitrile (pyridine-pyridinium bromide and phenol-sodium phenolate), whose ^s_spH can be derived from the Henderson-Hasselbach equation using the pKa values in acetonitrile reported for these systems.[58]

Synthesis

The neutral state of compounds **1**, **2** and **3** were prepared as previously reported, through a one-step method using picric acid and *N,N'*-diisopropylcarbodiimide (**1b**, 105 mg, yield: 35%),[37] 2,6-dinitro-4-(trifluoromethyl)phenol and *N,N'*-diisopropylcarbodiimide (tautomeric mixture of **2b+2c**, 65 mg, yield: 29%)[15], and picric acid and *N,N'*-dicyclohexylcarbodiimide (**3b**, 82 mg, yield: 22%).[41] Spectroscopic data for these compounds matched the previously reported data.[15,31,35] **1b**: ^{1}H NMR (360 MHz, CDCl$_3$): δ 9.01 (s, 2H), 4.30 (d, *J* = 9.0 Hz, 1H), 4.18 (sept, *J* = 6.6 Hz, 1H), 4.02 (m, 1H), 3.87 (sept, *J* = 7.2 Hz, 1H), 3.14 (sept, *J* = 6.9 Hz, 1H), 1.72 (d, *J* = 6.6 Hz, 6 H), 1.45 (d, *J* = 6.3 Hz, 6 H), 1.33 (d, *J* = 7.2 Hz, 6 H), 1.22 (d, *J* = 6.9 Hz, 6 H). **2b+2c**: ^{1}H NMR (400 MHz, CD$_3$CN, 298 K) δ 8.51 (s, 2H, **2c**), 8.19 (s, 2H, **2b**), 4.64 (m, 1H, **2b**), 4.53 (sept, *J* = 6.7 Hz, 1H, **2c**), 4.19 (sept, *J* = 6.6 Hz, 1H, **2b**), 3.97 (m, 1H, **2b**), 3.93-3.78 (m, 1H, **2b**, 1H, **2c**), 3.55-3.25 (m, 3H, **2c**), 3.19 (sept, *J* = 6.7 Hz, 1H, **2b**), 1.64 (d, *J* = 7.1 Hz, 6H, **2b**), 1.38 (d, *J* = 7.1 Hz, 6H, **2b**), 1.24 (d, *J* = 7.1 Hz, 6H, **2b**), 1.14 (d, *J* = 7.1 Hz, 6H, **2b**), 1.11 (d, *J* = 7.1 Hz, 12H, **2c**), 0.98 (d, *J* = 7.1 Hz, 6H, **2c**), 0.84 (m, 6H, **2c**). **3b**: ^{1}H NMR (360 MHz, CDCl$_3$): δ 9.03 (s, 2H), 4.53 (d, *J* = 9.0 Hz, 1H), 3.65 (tt, *J$_l$* = 11.7 Hz, *J$_l$* = 3.2 Hz, 1H), 3.48 (m, 1H), 3.29 (m, 1H), 2.64 (tt, *J$_l$* = 11.9 Hz, *J$_l$* = 3.6 Hz, 1H), 2.49 (q, *J* = 11.9 Hz, 2H), 2.34-1.50 (m, 20H), 1.43-0.92 (m, 18H).

Protonation of the neutral state of 1, 2 and 3

To generate the cationic states of **1**, **2** and **3**, the following general producedure was used. To a solution of the compound of interest (10 mg) in deuterated acetonitrile, trifluoroacetic acid was slowly added and the protonation process of **1b, 2b**+**2c** and **3b** was monitored by temperature dependent ^{1}H NMR and 2D COSY. **1d**: ^{1}H NMR (400 MHz, CD$_3$CN, 298 K): δ 9.07 (s, 2H), 7.25 (br s, 2H), 4.40 (sept, J = 6.5 Hz, 1H), 4.00 (sept, J = 6.5 Hz, 1H), 3.86 (br s, 2H), 1.35-1.15 (m, 18 H), 1.14 (d, J = 6.7 Hz, 6H). **2d**: ^{1}H NMR (400 MHz, CD$_3$CN, 298 K): δ 8.68 (s, 2H), 7.13 (br s, 1H), 6.85 (br s, 1H), 4.46 (sept, J = 6.6 Hz, 1H), 4.02 (sept, J = 6.5 Hz, 1H), 3.82 (br s, 2H), 1.35-1.10 (m, 24 H). **3d**: ^{1}H NMR (400 MHz, CD$_3$CN, 298 K): δ 9.06 (s, 2H), 7.20 (br s, 2H), 4.16 (t, J = 10.6 Hz, 1H), 3.84 (br s, 2H), 3.66 (t, J = 12.1 Hz, 1H), 1.90-1.45 (m, 8H), 1.40-0.80 (m, 32H).

Fabrication of electrofluorochromic ion gels

Electrofluorochromic ion gels were prepared following the procedure described in ref. 53 by codissolving 150 mg of 1-butyl-3-methylimidazolium bis(trifluoromethylsulfonyl)imide, 36 mg of poly(vinylidene fluoride-co-hexafluoropropylene, 9 mg of **1b** and, when necessary, 5 mg of 1,1'-dimethylferrocene in 3 mL of acetone. The mixture was fully dissolved after heating at 50 ºC for a few minutes. The solution was cast onto a glass slide and, after solvent evaporation, a flexible ion gel was obtained. The "cut-and-stick" strategy[53] was then followed to measure the electrochromic and electrofluorochromic behavior of the ion gels prepared, for which they were cut and the thin films obtained were sandwiched between two ITO-coated glass substrates that were fixed using double-sided tape.

Preparation of polymer thin films

Halochromic polymer films were prepared by dissolving 143 mg of PMMA (M$_w$=120000) in 5 mL of chloroform. Afterwards, 2 mg of **1b** were added to the mixture and the solution was

poured into a Petri dish (6 cm in diameter). The solution was left to evaporate over 2 hours at room temperature to obtain an orange fluorescent film (~ 1 mm in thickness). Acetonitrile-sensitive films were prepared by dissolving 150 mg of PS (M_w=350000) in 5 mL of chloroform upon sonication. Afterwards, 2 mg of the tautomerix mixture **2b**+**2c** were added to the mixture and the solution was poured into a Petri dish (6 cm in diameter). The solution was left to evaporate over 2 hours at room temperature to obtain a homogeneous, almost colourless PS film (~ 1 mm in thickness). Another set of acetonitrile-sensitive films were prepared by dissolving 93 mg of PVA (M_w=125000) in 5 mL of hot water. To this mixture, 200 µL of a 0.25 mM solution of the mixture **2b**+**2c** in acetonitrile were added. The solution was then poured into a glass Petri plate (6 cm in diameter) and water was left to evaporate overnight at room temperature to obtain a homogenous, slightly purple PVA film (~ 1 mm in thickness).

ACKNOWLEDGMENTS

SUPPORTING INFORMATION

Additional spectroscopic data about SZMC switches **1-3** is provided in the Supporting Information (Figures S1-S5 and Table S1).

REFERENCES

[1] de Silva, A. P.; Gunaratne, H. Q. N.; Gunnlaugsson, T.; Huxley, A. J. M.; McCoy, C. P.; Rademacher, J. T.; Rice, T. E. Signaling Recognition Events with Fluorescent Sensors and Switches. *Chem. Rev.* **1997**, 97, 1515-1566.

[2] Wu, J.; Liu, W.; Ge, J.; Zhang, H.; Wang, P. New Sensing Mechanisms for Design of Fluorescent Chemosensors Emerging in Recent Years. *Chem. Soc. Rev.* **2011**, 40, 3483-3495.

[3] Lou, Z.; Li, P.; Han, K. Redox-Responsive Fluorescent Probes with Different Design Strategies. *Acc. Chem. Res.* **2015**, 48, 1358-1368.

[4] Wei, H.; Zhang, J.; Shi, N.; Liu, Y.; Zhang, B.; Wan, X. A Recyclable Polyoxometalate-Based Supramolecular Chemosensor for Efficient Detection of Carbon Dioxide. *Chem. Sci.* **2015**, 6, 7201-7205.

[5] Kobayashi, H.; Ogawa, M.; Alford, R.; Choyke, P. L.; Urano, Y. New Strategies for Fluorescent Probe Design in Medical Diagnostic Imaging. *Chem. Rev.* **2010**, 110, 2620-2640.

[6] Yang, Z.; Sharma, A.; Qi, J.; Peng, X.; Lee, D. Y.; Hu, R.; Lin, D.; Qu, J.; Kim, J. S. Super-resolution Fluorescent Materials: an Insight into Design and Bioimaging Applications. *Chem. Soc. Rev.* **2016**, 45, 4651-4667.

[7] Yu, F.; Li, P.; Li, G.; Zhai, G.; Chu, T.; Han, K. A Near-IR Reversible Fluorescent Probe Modulated by Selenium for Monitoring Peroxynitrite and Imaging in Living Cells. *J. Am. Chem. Soc.* **2011**, 133, 11030-11033.

8   Yu, F.; Li, P.; Wang, B.; Han, K. Reversible Near-Infrared Fluorescent Probe Introducing Tellurium to Mimetic Glutathione Peroxidase for Monitoring the Redox Cycles between Peroxynitrite and Glutathione in Vivo. *J. Am. Chem. Soc.* **2013**, 135, 7674-7680.

9   Irie, M.; Fukaminato, T.; Sasaki, T.; Tamai, N.; Kawai, T. Organic Chemistry: a Digital Fluorescent Molecular Photoswitch. *Nature*, **2002**, 420, 759-760.

10   Berberich, M.; Krause, A. M.; Orlandi, M.; Scandola, F.; Würthner, F. Toward Fluorescent Memories with Nondestructive Readout: Photoswitching of Fluorescence by Intramolecular Electron Transfer in a Diaryl Ethene Perylene Bisimide Photochromic System. *Angew. Chem. Int. Ed.* **2008**, 47, 6616-6619.

11   de Silva, A. P.; Uchiyama, S. Molecular Logic and Computing. *Nat. Nanotech.* **2007**, 2, 399-410.

12   Andréasson, J.; Pischel, U. Molecules with a Sense of Logic: a Progress Report. *Chem. Soc. Rev.* **2015**, 44, 1053-1069.

13   Sarkar, T.; Selvakumar, K.; Motiei, L.; Margulies, D. Message in a Molecule. *Nat. Commun.* **2016**, 7, 11374.

14   Majumdar, T.; Haldar, B.; Mallick, A. A Strategic Design of an Opto-Chemical Security Device with Resettable and Reconfigurable Password Based Upon Dual Channel Two-in-One Chemosensor Molecule. *Sci. Rep.* **2017**, 7, 42811.

15   Gallardo, I.; Guirado, G.; Hernando, J.; Morais, S.; Prats, G. A Multi-Stimuli Responsive Switch as a Fluorescent Molecular Analogue of Transistors. *Chem. Sci.* **2016**, 7, 1819-1825.

[16] Zheng, R.; Mei, X.; Lin, Z.; Zhao, Y.; Yao, H.; Lv, W.; Ling, Q. Strong CIE Activity, Multi-Stimuli-Responsive Fluorescence and Data Storage Application of New Diphenyl Maleimide Derivatives. *J. Mater. Chem. C* **2015**, 3, 10242-10248.

[17] Yoon, S.-J.; Chung, J. W.; Gierschner, J.; Kim, K. S.; Choi, M.-G.; Kim, D.; Park, S. Y. Multistimuli Two-Color Luminescence Switching via Different Slip-Stacking of Highly Fluorescent Molecular Sheets. *J. Am. Chem. Soc.* **2010**, 132, 13675-13683.

[18] Lu, X.-L.; Xia, M. Multi-Stimuli Response of a Novel Half-Cut Cruciform and its Application as a Security Ink. *J. Mater. Chem. C* **2016**, 4, 9350-9358.

[19] Chen, P.; Li, Q.; Grindy, S.; Holten-Andersen, N. White-Light-Emitting Lanthanide Metallogels with Tunable Luminescence and Reversible Stimuli-Responsive Properties. *J. Am. Chem. Soc.* **2015**, 137, 11590-11593.

[20] Liu, L.; Wang, X.; Wang, N.; Peng, T.; Wang, S. Bright, Multi responsive, Sky Blue Platinum(II) Phosphors Based on a Tetradentate Chelating Framework. *Angew. Chem. Int. Ed.* **2017**, 56, 9160-9164.

[21] Shen, J.; Pang, J.; Kalwarczyk, T.; Holyst, R.; Xin, X.; Xu, G.; Luan, X.; Yang, Y. Manipulation of Multiple-Responsive Fluorescent Supramolecular Materials Based on the Inclusion Complexation of Cyclodextrins with Tyloxapol. *J. Mater. Chem. C* **2015**, 3, 8104-8113.

22 Shen, J.; Wang, Z.; Sun, D.; Xia, C.; Yuan, S.; Sun, P.; Xin, X. pH-Responsive Nanovesicles with Enhanced Emission Co-Assembled by Ag(I) Nanoclusters and Polyethyleneimine as a Superior Sensor for Al^{3+}. *ACS Appl. Mater. Interfaces* **2018**, 10, 3955-3963.

23 de Silva, A. P. Analytical Chemistry: Sense and Versatility. *Nature* **2007**, 445, 718-719.

24 Chhatwal, M.; Kumar, A.; Singh, V.; Gupta, R. D.; Awasthi, S. K. Addressing of Multiple-Metal Ions on a Single Platform. *Coord. Chem. Rev.* **2015**, 292, 30-55.

25 Hariharan, P. S.; Venkataramanan, N. S.; Moon, D.; Anthony, S. P. Self-Reversible Mechanochromism and Thermochromism of a Triphenylamine-Based Molecule: Tunable Fluorescence and Nanofabrication Studies. *J. Phys. Chem. C* **2015**, 119, 9460-9469.

26 Browne, W. R.; Pollard, M. M.; de Lange, B.; Meetsma, A.; Feringa, B. L. Reversible Three-State Switching of Luminescence: A New Twist to Electro- and Photochromic Behavior. *J. Am. Chem. Soc.* **2006**, 128, 12412-12413.

27 Zhou, W.; Li, J.; He, X.; Li, C.; Lv, J.; Li, Y.; Wang, S.; Liu, H.; Zhu, D. A Molecular Shuttle for Driving a Multilevel Fluorescence Switch. *Chem. Eur. J.* **2008**, 14, 754-763.

28 Evangelio, E.; Hernando, J.; Imaz, I.; Bardají, G. G.; Alibés, R.; Busqué, F.; Ruiz-Molina, D. Catechol Derivatives as Fluorescent Chemosensors for Wide Range pH Detection. *Chem. Eur. J.* **2008**, 14, 9754-9763.

29 Gu, H.; Bi, L.; Fu, Y.; Wang, N.; Liu, S.; Tang, Z. Multistate Electrically Controlled Photoluminescence Switching. *Chem. Sci.* **2013**, 4, 4371-4377.

[30] Bill, N. L.; Lim, J. M.; Davis, C. M.; Bähring, S.; Jeppesen, J. O.; Kim, D.; Sessler, J. L. π-Extended Tetrathiafulvalene BODIPY (ex-TTF-BODIPY): a Redox Switched "on–off–on" Electrochromic System with Two Near-Infrared Fluorescent Outputs. *Chem. Commun.* **2014**, 50, 6758-6761.

[31] Gallardo, I.; Guirado, G. Electrochemical Mechanism of Spiro and Zwitterionic Meisenheimer Compounds: A Potential Fluorescence Molecular Switching System. *Electrochem. Commun.* **2007**, 9, 173-179.

[32] Al-Kaysi, R. O.; Bourdelande, J. L.; Gallardo, I.; Guirado, G.; Hernando, J. Investigation of an Acid–Base and Redox Molecular Switch: From Bulk to the Single Molecule Level. *Chem. Eur. J.* **2007**, 13, 7066-7074.

[33] Al-Kaysi, R. O.; Gallardo, I.; Guirado, G. Stable Spirocyclic Meisenheimer Complexes. *Molecules* **2008**, 13, 1282-1302.

[34] Sala, N.; Prats, G.; Villabona, M.; Gallardo, I.; Hamdan, T.; Al-Kaysi, R. O.; Hernando, J.; Guirado, G. New Smart Functional Fluorophores Based on Stable Spirocyclic Zwitterionic Meisenheimer Compounds. *Dyes Pigm.* **2018**, 153, 160-171.

[35] Terrier. F. Nucleophilic Aromatic Displacement: The Influence of the Nitro Group, Feuer, H. editor. New York: VCH Publishers, **1991**.

[36] Terrier, F. Rate and Equilibrium Studies in Jackson-Meisenheimer Complexes. *Chem. Rev.* **1982**, 82, 77-152.

37 Al-Kaysi, R. O.; Guirado, G.; Valente, E. J. Synthesis and Characterization of a New Fluorescent Zwitterionic Spirocyclic Meisenheimer Complex of 1,3,5 Trinitrobenzene. *Eur. J. Org. Chem.* **2004**, 3408-3411.

38 Al-Kaysi, R. O.; Mueller, A. M.; Ahn, T. S.; Lee, S.; Bardeen, C. J. Effects of Sonication on the Size and Crystallinity of Stable Zwitterionic Organic Nanoparticles Formed by Reprecipitation in Water. *Langmuir* **2005**, 21, 7990-7994.

39 Das, T.; Haldar, A. Pramanik and D. On-line Ammonia Sensor and Invisible Security Ink by Fluorescent Zwitterionic Spirocyclic Meisenheimer Complex. *Sci. Rep.* **2017**, 7, 40465.

40 Das, T.; Haldar, D. Mopping up the Oil, Metal, and Fluoride Ions from Water. *ACS Omega* **2017**, 2, 6878-6887.

41 Benet, M.; Villabona, M.; Llavina, C.; Mena, S.; Hernando, J.; Al-Kaysi, R. O.; Guirado, G. Fluorescent "Turn-Off" Detection of Fluoride and Cyanide Ions Using Zwitterionic Spirocyclic Meisenheimer Compounds. *Molecules* **2017**, 22, 1842.

42 Dasary, S. S. R.; Singh, A. K.; Lee , K. S.; Yu, H.; Ray, P. C. A Miniaturized Fiber-Optic Fluorescence Analyzer for Detection of Picric-Acid Explosive from Commercial and Environmental Samples. *Sens. Act. B Chem.* **2018**, 255, 1646-1654.

43 de Silva, A. P.; de Silva, S. S. K.; Goonesekera, N. C. W.; Gunaratne, H. Q. N.; Lynch, P. L.; Nesbitt, R. K.; Patuwathavithana, S. T.; Ramyalai, N. L. D. Analog Parallel Processing of Molecular Sensory Information. *J. Am. Chem. Soc.* **2007**, 129, 3050-3051.

44 Wencel, D.; Abel, T.; McDonagh, C. Optical Chemical pH Sensors. *Anal. Chem.* **2014**, 86, 15-29.

45 Rondinini, S. pH Measurements in Non-Aqueous and Aqueous-Organic Solvents – Definition of Standard Procedures. *Anal. Bional. Chem.* **2002**, *374*, 813-816.

46 Thompson, B. C.; Winther-Jensen, O.; Winther-Jensen, B.; MacFarlane, D. R. A Solid-State pH Sensor for Nonaqueous Media Including Ionic Liquids. *Anal. Chem.* **2013**, *85*, 3521-3525.

47 Brown, R. J. C.; Keates, A. C.; Brewer, P. J. Sensitivities of a Standard Test Method for the Determination of the pHe of Bioethanol and Suggestions for Improvement. *Sensors* **2010**, *10*, 9982-9993.

48 Kolthoff, I. M.; , M. K. Chantooni Jr. Autoprotolysis Constant of Acetonitrile. *J. Phys. Chem.* **1968**, 72, 2270-2272.

49 Ferreira, R.; Remón, P.; Pischel, U. Multivalued Logic with a Tristable Fluorescent Switch. *J. Phys. Chem. C* **2009**, *113*, 5805-5811.

50 Pais, V. F.; Lineros, M.; López-Rodríguez, R.; El-Sheshtawy, H. S. Fernández, R.; Lassaletta, J. M.; Ros, A.; Pischel, U. Preparation and pH-Switching of Fluorescent Borylated Arylisoquinolines for Multilevel Molecular Logic. *J. Org. Chem.* **2013**, *78*, 7949-7961.

51 M'Halla, F.; Pinson, J.; Savéant, J. M. The Solvent as H-Atom Donor in Organic Electrochemical Reactions. Reduction of Aromatic Halides. *J. Am. Chem. Soc.* **1980**, *102*, 4120-4127.

52 Krishnan, A. T.; Chakravarthi, S.; Nicollian, P.; Reddy, V.; Krishnan, S. Negative Bias Temperature Instability Mechanism: The Role of Molecular Hydrogen. *Appl. Phys. Lett.* **2006**, *88*, 153518.

53 Moon, H. C.; Kim, C.-H.; Lodge, T. P.; Frisbie, C. D. Multicolored, Low-Power, Flexible Electrochromic Devices Based on Ion Gels. *ACS Appl. Mater. Interfaces* **2016**, 8, 6252-6260.

54 Reichardt, C. Solvatochromic Dyes as Solvent Polarity Indicators. *Chem. Rev* **1994**, *94*, 2319-2358.

55 Lakowicz, J.R. Principles of Fluorescence Spectroscopy, Springer, NewYork, USA, **2006**.

56 Kircher, T.; Löhmannsröben, H.-G. Photoinduced Charge Recombination Reactions of a Perylene Dye in Acetonitrile. *Phys. Chem. Chem. Phys.* **1999**, 1, 3987-3992.

57 Sánchez, R. S.; Gras-Charles, R.; Bourdelande, J. L.; Guirado, G.; Hernando, J. Light- and Redox-Controlled Fluorescent Switch Based on a Perylenediimide–Dithienylethene Dyad. *J. Phys. Chem. C* **2012**, 116, 7164-7172.

58 Espinosa, S.; Bosch, E.; Rosés, M. Retention of Ionizable Compounds on HPLC. 5. pH Scales and the Retention of Acids and Bases with Acetonitrile−Water Mobile Phases. *Anal. Chem.* **2000**, 72, 5193-5200.

Supporting Information

Multistimuli-Responsive Fluorescent Switches Based on Spirocyclic Meisenheimer Compounds: Smart Molecules for the Design of Optical Probes and Electrochromic Materials

Marc Villabona,[a] Marina Benet,[a] Silvia Mena,[a] Rabih O. Al-Kaysi,[b] Jordi Hernando[a] and Gonzalo Guirado*[a]*

[a] Departament de Química, Universitat Autònoma de Barcelona, Facultat de Ciències, 08193, Cerdanyola del Vallès, Spain

[b] College of Science and Health Professions, King Saud bin Abdulaziz University for Health Sciences, and King Abdullah International Medical Research Center, Ministry of National Guard Health Affairs, Riyadh 11426, Kingdom of Saudi Arabia.

E-mail: jordi.hernando@uab.cat, gonzalo.guirado@uab.cat

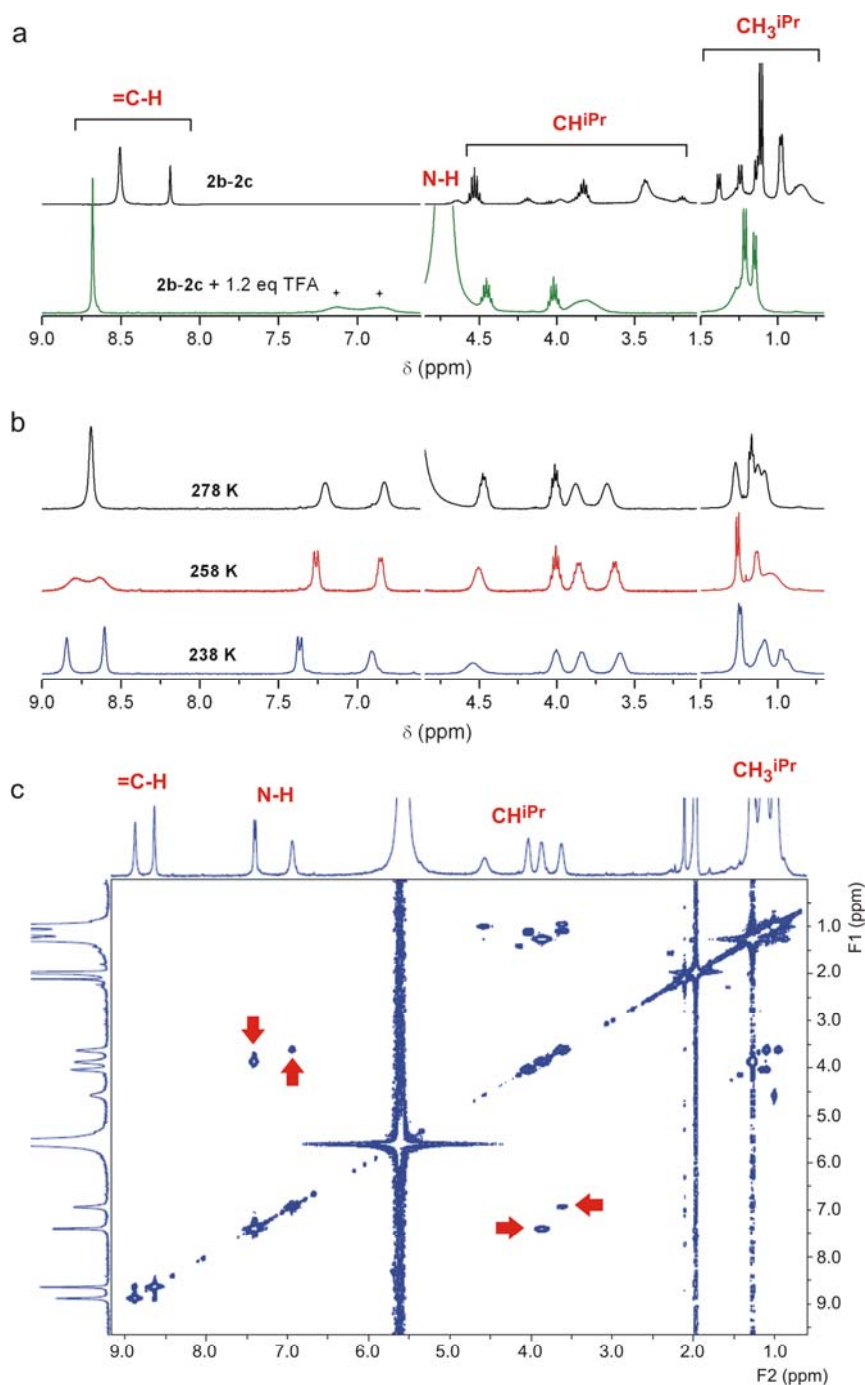# TABLE OF CONTENTS

1. Protonation of SZMC switch 2

Figure S1. (a) Variation of the ^{1}H NMR (400 MHz, CD$_3$CN, 298 K) spectrum of the tautomeric mixture **2b+2c** upon addition of 1.20 equivalents of TFA, which leads to the quantitative formation of the protonated state **2d**. Black stars are used to indicate the formation of two new signals corresponding to the two NH groups of **2d**. (b) Variation of the ^{1}H NMR (400 MHz, CD$_3$CN) spectrum of **2d** with

temperature, which allows resolving the signals for the two different NH groups of the compound at $\delta \sim$ 7.00 ppm. (c) 2D COSY spectrum (400 MHz, CD$_3$CN, 238 K) of **2d**, where cross-peaks are observed between each of the NH resonances at δ~6.90 and 7.35 ppm and the isopropyl CH multiplets at $\delta \sim$ 4.00 and 3.60 ppm (CH^{iPr}). For sake of clarity, the intensity of the ^{1}H NMR signals in the region 9.0 – 3.1 ppm (x6) were amplified in the spectra of (a) and (b).

2. Protonation of SZMC switch 3

To establish the structure of the cation obtained upon protonation of zwitterion **3b**, we monitored the titration of **3b** with trifluoroacetic acid (TFA) by ^{1}H NMR. In this case, we used deuterated dimethylformamide as a solvent since: (a) it allowed direct monitorization of the new proton introduced into the system along the process, and (b) **3b** was found to be poorly soluble in deuterated acetonitrile, in contrast to **1b** and **2b**. As shown in Figure S2a, gradual disappearance of the most characteristic ^{1}H NMR signals of **3b** was observed upon addition of TFA, such as those arising from the cyclohexadienyl anion protons ($\delta = 8.89$ ppm), the guanidinium NH moiety ($\delta = 5.95$ ppm) and the CH group of the cyclohexyl substituents ($\delta = 3.83, 3.58, 3.31$ and 2.82 ppm). In addition, a new set of resonances corresponding to the protonation product concomitantly appeared between $\delta \sim 9.6\text{-}9.0$ ppm and $\sim 4.2\text{-}3.3$ ppm (Figure S2a). It is worth noting that complete fading of the ^{1}H NMR signals of **3b** was observed upon addition of *ca.* 1.2 equivalents of TFA, thus indicating quantitative conversion into a new species. As previously observed for **1b** and **2b**, this resulted in sample discoloration, which revealed that the 2,4,6-trinitrocyclohexadienyl anion chromophore of **3b** had been disrupted upon TFA addition and, therefore, was not longer present in the protonated product.

The loss of the chromophore unit of **3b** could be explained on the basis of two different processes: (a) protonation-induced ring-opening reaction of **3b**, which would lead to an aromatic structure by analogy to the results obtained for **1b** and **2b** (structure **3d** in Figure S3); (b) C4-protonation of the cyclohexadienyl anion, which would preserve the spirocyclic structure of the system, as proposed by Das and co-workers when conducting the experiment in CDCl$_3$ (structure **3d'** in Figure S3).[1] To discriminate between structures **3d** and **3d'**, we performed two additional ^{1}H NMR experiments: (a) temperature variable ^{1}H NMR spectroscopy of the cationic state of **3** within the 318-258 K range (Figure S2b); (b) 2D COSY spectroscopy of this compound at 288 K (Figure S2c). When analyzing these new spectra, we particularly focused our attention on the four ^{1}H NMR signals of equal intensity detected between $\delta \sim 9.6\text{-}9.0$ ppm. Since cyclohexyl groups cannot provide ^{1}H NMR resonances at such

low fields, these signals must correspond to H3, H5, NH and the new proton introduced upon TFA addition for any of the two structures proposed for the cationic state of **3**.

The most significant effect observed at low fields in temperature variable measurements was the broadening and coalescence of the ^{1}H NMR signals at $\delta \sim 9.5$ and 9.3 ppm when heating up. More importantly, correlation was observed between those two resonances in the 2D COSY spectrum at 288 K, and they did not show cross peaks with any other nucleus in the molecule (Figure S2c). Based on these features, we assigned the ^{1}H NMR signals at $\delta \sim 9.5$ and 9.3 ppm to the two aromatic protons H3 and H5 in structure **3d**, which should become anisochronous if the rotation around the bulky urea substituent sufficiently slows down when cooling, as also described for analogue compound **2c**.[2] Noticeably, if those two signals had arisen from structure **3d'**, additional cross-peaks would have been found in the 2D COSY spectrum with the new proton H4 introduced in this compound.

On the other hand, clear doublet multiplicities were observed at 298-288 K for resonances at $\delta \sim 9.2$ and 9.0 ppm, which are in agreement with those expected for the two NH groups of structure **3d**. This assignment is further corroborated by the 2D COSY spectrum registered at 288 K, where crossed peaks were observed between each of those doublets and two different CH protons of the cyclohexyl groups at $\delta \sim 3.7$ and 3.5 ppm (Figure S2c). These results would not have been possible for structure **3d'**, where correlation with cyclohexyl CH protons would have not been observed for H4, but only for NH (i.e. only for one of the resonances at δ ~9.6-9.0 ppm).

In conclusion, our ^{1}H NMR analysis of **3b** protonation allows clear disambiguation of the actual structure of the cationic state of the system: the new proton introduced cannot be attached to the unsaturated ring of the compound, but it must lie next to a cyclohexyl substituent, as proposed in our work (**3d**) and in contrast to the assignment of Das and co-workers (**3d'**).[1]
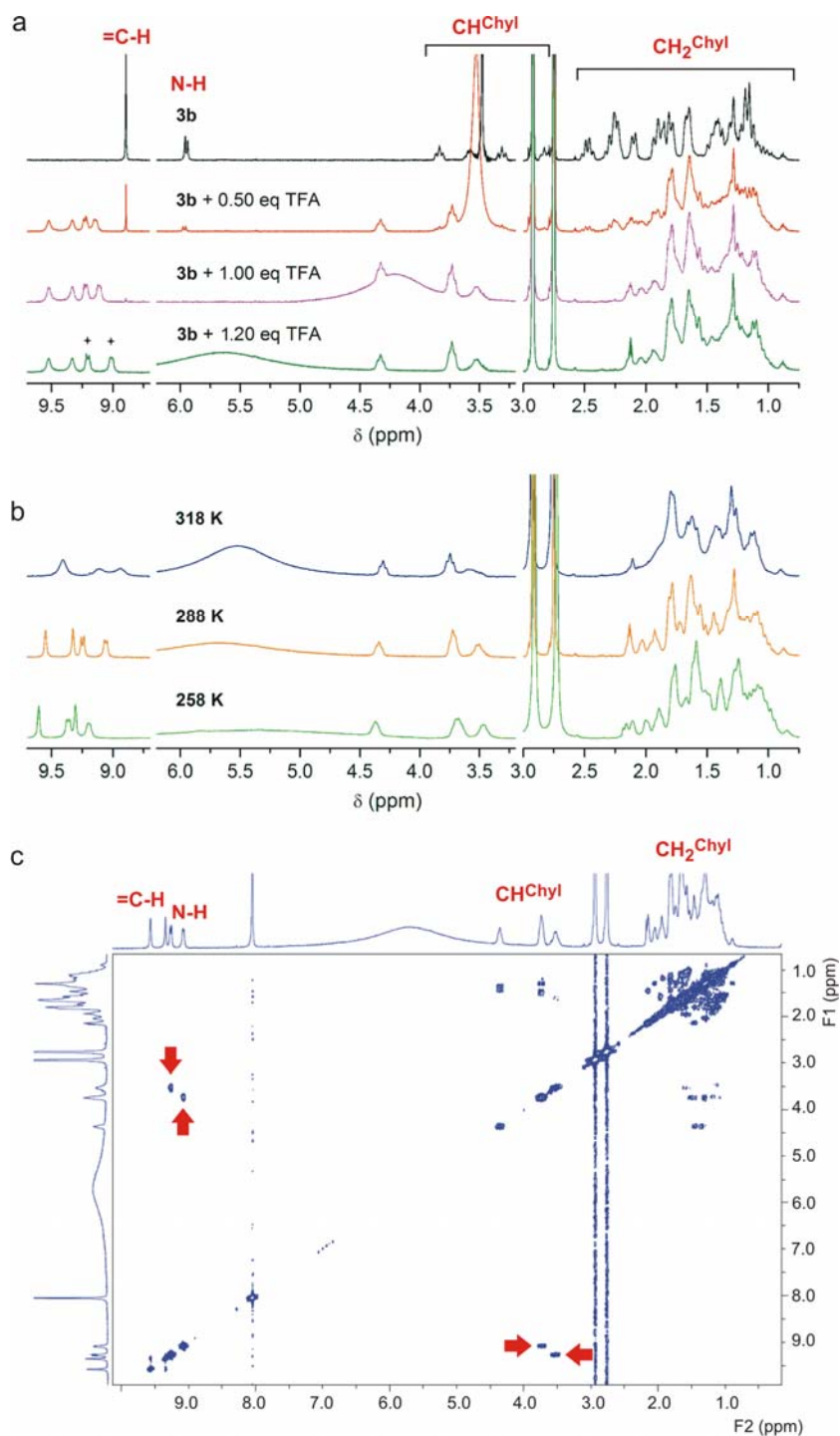
Figure S2. (a) Variation of the ^{1}H NMR (400 MHz, DMF-d_7, 298 K) spectrum of **3b** upon addition of 1.2 equivalents of TFA, which leads to the quantitative formation of a new protonated state that we assigned to structure **3d** (see Figure S3). Black stars are used to indicate the formation of two new signals corresponding to the two NH groups of **3d**. (b) Variation of the ^{1}H NMR (400 MHz, DMF-d_7)

spectrum of **3d** with temperature. c) 2D COSY spectrum (400 MHz, DMF-d_7, 288 K) of **3d**, where cross-peaks are observed between each of the NH resonances at $\delta \sim 9.2$ and 9.0 ppm and the cyclohexyl CH multiplets at $\delta \sim 3.7$ and 3.5 ppm (CH$^{\text{Chyl}}$).
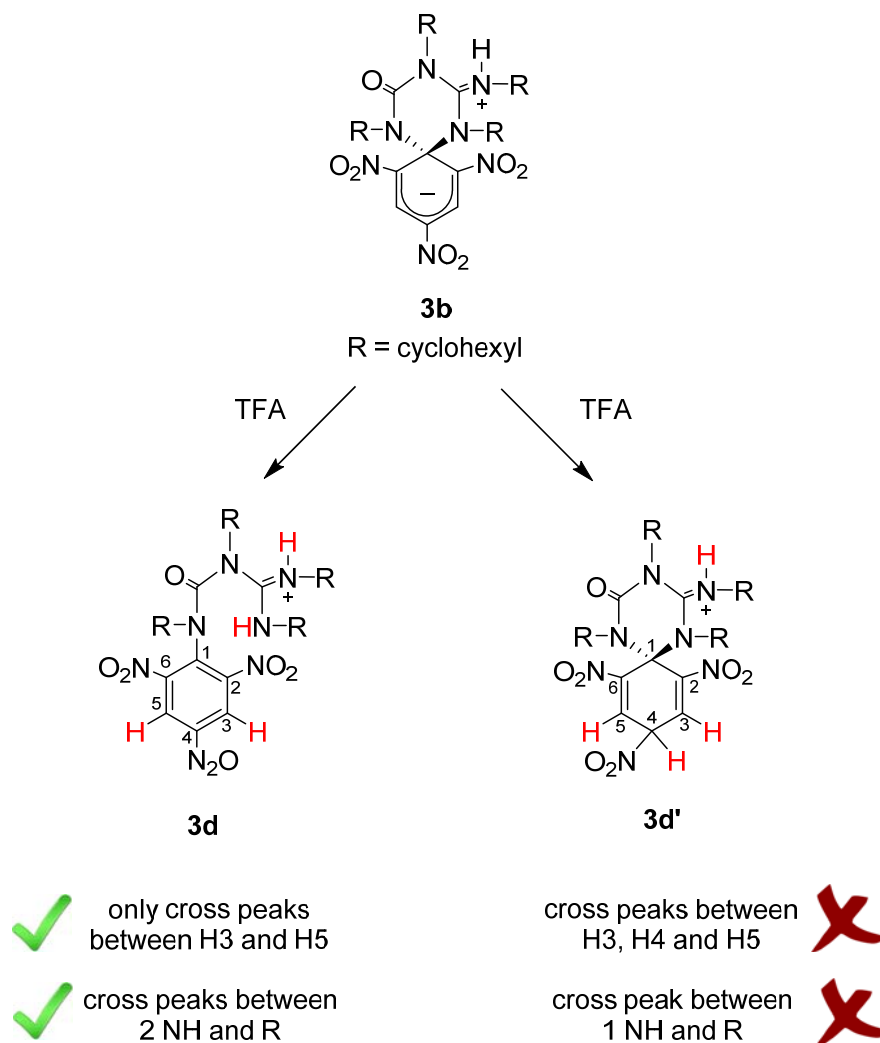

Figure S3. Two possible structures proposed for the cationic state of **3**: structure **3d** (this work) and structure **3d'** (Das and co-workers).[1] For each structure, the main 2D COSY spectral features expected are indicated, which allow discrimination between **3d** and **3d'**.
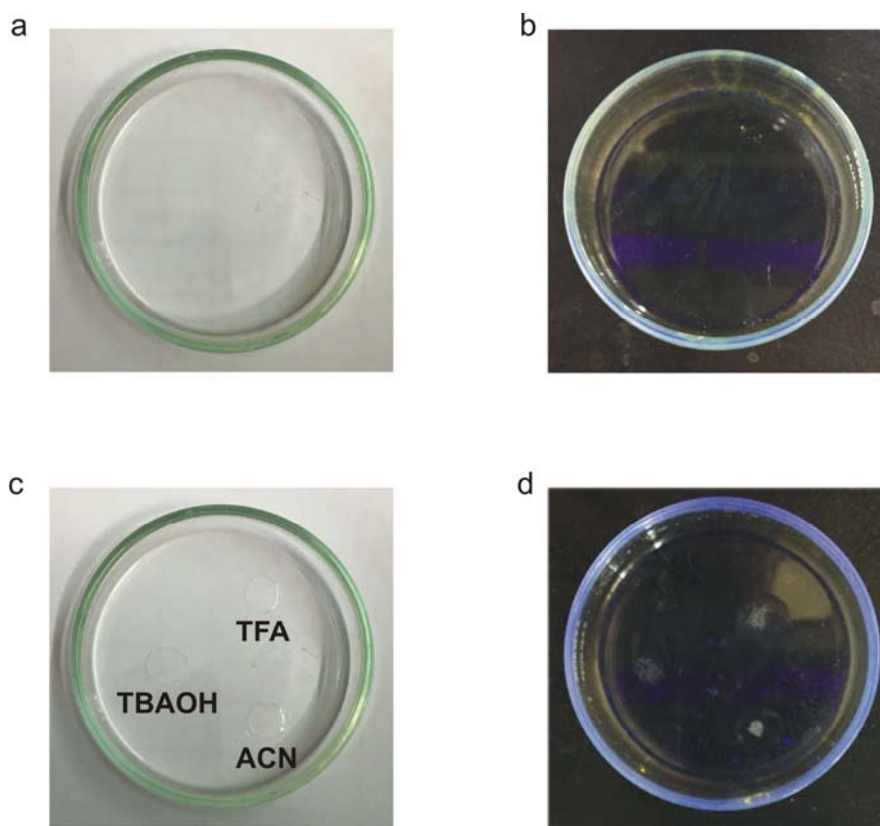
3. pH response of pure PMMA films

Figure S4. (a-b) Photographs of a pure PMMA film deposited onto a glass Petri dish. The image in (b) was taken in the dark and under irradiation with a 365 nm lamp to detect any possible residual emission arising from the PMMA film or the Petri dish. (c-d) Photographs of the same PMMA film after depositing droplets of 3 different solutions: acetonitrile (ACN), a 0.1 M TFA acetonitrile solution (TFA), and a 0.1 M TBAOH acetonitrile solution (TBAOH). The image in (d) was taken in the dark and under irradiation with a 365 nm lamp.

4. Solvent dependence on the tautomeric equilibrium between 2b and 2c

As already established in a previous work,[2] the relative concentration between the spirocyclic zwitterion **2b** and the aromatic neutral tautomer **2c** can be estimated from the integrals of the ^{1}H NMR signals arising from their cyclohexadienyl (for **2b**) and aromatic (for **2c**) protons, which appear in the low field region of the spectrum. To illustrate this procedure, Figure S4 plots these ^{1}H NMR signals for two of the solvents considered (acetone-d_6 and methanol-d_4) at 273, 298 and 313 K.
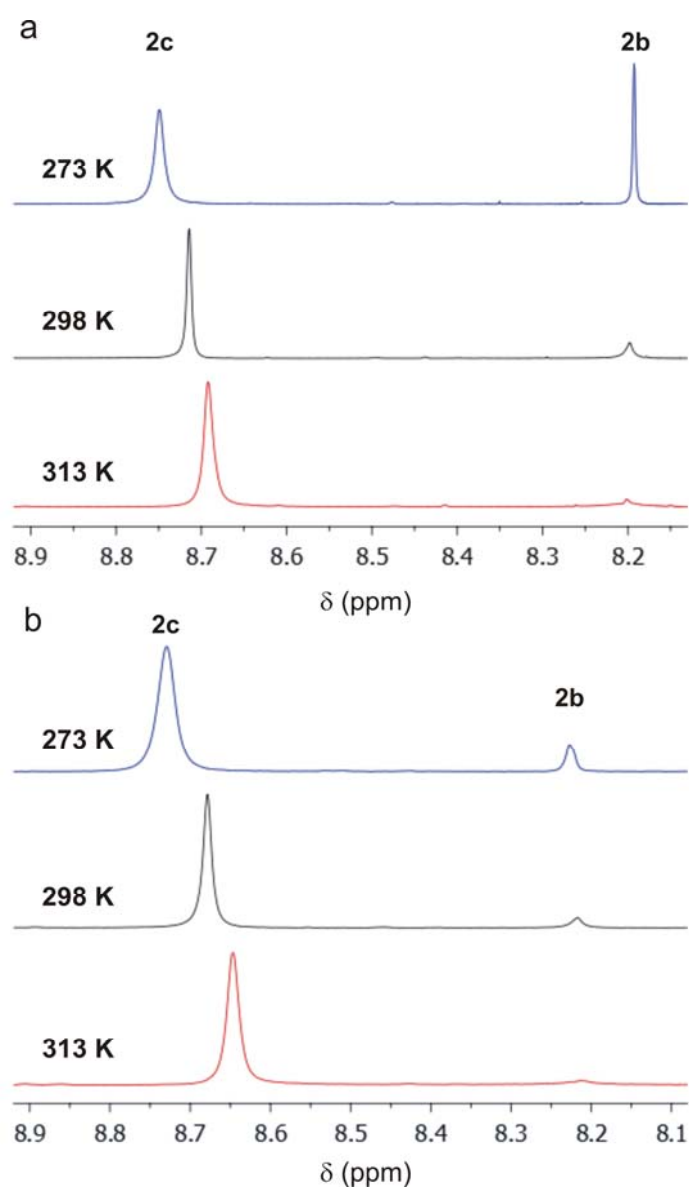

Figure S5. Low field region of the ^{1}H NMR spectrum (400 MHz) of an equilibrium mixture of tautomers **2b** and **2c** in: (a) acetone-d_6, and (b) methanol-d_4.

Table S1. Fluorescence quantum yield of **2b** in different solvents at 298 K

Solvent	$\varepsilon^{\,a}$	Φ_{fl}
Toluene	2.38	0.71
CHCl$_3$	4.82	0.84
CH$_2$Cl$_2$	10.36	0.85
THF	7.58	0.85
Acetone	20.7	0.77
ACN	37.5	0.76
DMSO	46.7	0.65
MeOH	32.7	0.40
H$_2$O	80.1	0.11

[a] Dielectric constant of the solvent.

5. References

[1] Das, T.; Haldar, A. Pramanik and D. On-line Ammonia Sensor and Invisible Security Ink by Fluorescent Zwitterionic Spirocyclic Meisenheimer Complex. *Sci. Rep.* **2017**, 7, 40465.

[2] I Gallardo, I.; Guirado, G.; Hernando, J.; Morais, S.; Prats, G. A Multi-Stimuli Responsive Switch as a Fluorescent Molecular Analogue of Transistors. *Chem. Sci.* **2016**, 7, 1819-1825.